

# **Fate of High Priority Pesticides During Drinking Water Treatment**

EPA/600/R-08/089  
September 2008

# **Fate of High Priority Pesticides During Drinking Water Treatment**

by

Stephen E. Duirk, <sup>†</sup>Lisa M. Desetto, and <sup>†</sup>Gary M. Davis  
National Exposure Research Laboratory  
Ecosystems Research Division  
Athens, GA

<sup>†</sup>Student Services Authority

U.S. Environmental Protection Agency  
Office of Research and Development  
Washington D.C. 20460

## **NOTICE**

This work has been subject to external peer and administrative review, and has been approved for publication as an EPA document. Mention of trade names or commercial products does not constitute endorsement or recommendation for use.

## ABSTRACT

The fate of organophosphorus (OP) pesticides in the presence of chlorinated oxidants was investigated under drinking water treatment conditions. In the presence of aqueous chlorine, intrinsic rate coefficients were found for the reaction of hypochlorous acid ( $k_{\text{HOCl,OP}}$ ) and hypochlorite ion ( $k_{\text{OCl,OP}}$ ) with eight OP pesticides. The reaction of hypochlorous acid (HOCl) with each OP pesticide was relatively rapid at near neutral pH,  $k_{\text{HOCl,OP}} = 0.86 - 3.56 \times 10^6 \text{ M}^{-1}\text{h}^{-1}$ . The reaction of HOCl with OP pesticides occurs at the thiophosphate (P=S) moiety resulting in the formation of the corresponding oxon (P=O), which is more toxic than the parent OP pesticide. Hypochlorite ion ( $\text{OCl}^-$ ) was found not to oxidize the pesticide but act like a nucleophile accelerating hydrolysis,  $k_{\text{OCl,OP}} = 37.3 - 15,908.9 \text{ M}^{-1}\text{h}^{-1}$ . Both the  $k_{\text{HOCl,OP}}$  and the  $k_{\text{OCl,OP}}$  were found to correlate well with molecular descriptors within each subgroup of OP pesticide class. The most commonly detected OP pesticides in drinking water sources were then investigated in the presence of monochloramine ( $\text{NH}_2\text{Cl}$ ). Monochloramine was found not to be very reactive with OP pesticides,  $k_{\text{NH}_2\text{Cl,OP}} = 10.6 - 21.4 \text{ M}^{-1}\text{h}^{-1}$ . Dichloramine ( $\text{NHCl}_2$ ) was found to be two orders of magnitude more reactive with the OP pesticides investigated than monochloramine,  $k_{\text{NHCl}_2,\text{OP}} = 1995.0 - 2931.9 \text{ M}^{-1}\text{h}^{-1}$ . The reactivity of the three chlorinated oxidants was then found to correlate with half-wave potentials ( $E_{1/2}$ ) for each OP pesticide respectively. A model was developed to predict the transformation of OP pesticides in the presence of chlorinated oxidants. With hydrolysis rate coefficients, the transformation of OP pesticides under drinking water treatment condition was found to be adequately predicted over the pH range of 6.5-9. The structure-activity relationships and mechanistic models developed here could be used by regulators to determine if drinking potable water contaminated with OP pesticides represents significant risk to a receiving population serviced by a community water system.

## ACKNOWLEDGEMENT

The authors would like to thank Mr. Jimmy Avants and Dr. Lidia Samarkina their technical assistance, Dr. Paul Winget for calculating highest occupied molecular orbital ( $E_{\text{HOMO}}$ ) energies for the organophosphorus pesticides, Dr. Wayne Garrison and Dr. Jackson Ellington for their consultation and expertise, as well as Dr. Craig Adams at the Missouri University of Science and Technology and Dr. David Sedlak at the University of California, Berkeley for agreeing to review this report. Finally, the authors would like to thank Dr. Mac Long and Dr. Eric Weber for their continued support of this work at the Ecosystems Research Division in Athens, GA.

## TABLE OF CONTENTS

LIST OF TABLES .....	v
LIST OF FIGURES .....	vi
EXECUTIVE SUMMARY .....	ix
1 INTRODUCTION .....	1
2 EXPERIMENTAL PROCEDURES .....	5
2.1 Materials .....	5
2.2 Methods.....	5
2.2.1 Chlorination and Hydrolysis of OP Pesticides.....	5
2.2.2 Chloramination of OP Pesticides .....	7
2.3 OP Pesticide Analysis .....	8
2.4 Numerical Calculations and Parameter Estimation .....	8
3 RESULTS AND DISCUSSION .....	9
3.1 Hydrolysis of select OP pesticides.....	9
3.2 OP Pesticide Degradation in the Presence of Aqueous Chlorine .....	11
3.3 OP Oxon Chlorine-Assisted Hydrolysis .....	16
3.4 OP Pesticide-Chlorine Model Validation .....	17
3.5 OP Pesticide Degradation in the Presence of Monochloramine .....	17
4 CONCLUSION.....	24
5 REFERENCES .....	27
TABLES .....	31
FIGURES .....	39

## LIST OF TABLES

Table 1	Stoichiometric equations and coefficients in the monochloramine autodecomposition model.....	32
Table 2	Structures and some chemical properties of select OP Pesticides (48). ....	33
Table 3	Neutral and alkaline hydrolysis rate coefficients for 8 OP pesticides and 3 oxon transformation products. 95% confidence intervals shown in parentheses. ....	34
Table 4	Stoichiometric equations used in the chlorine-OP pesticide transformation pathway model.....	35
Table 5	Oxidation and chlorine-assisted hydrolysis rate coefficients for 8 OP pesticides and 3 oxon transformation products. 95% confidence intervals shown in parentheses. ....	36
Table 6	Differential equations for the monochloramine autodecomposition model. ....	37
Table 7	Intrinsic rate coefficients for monochloramine and dichloramine reacting with CP, DZ, and MA. 95% confidence intervals shown in parentheses. ....	38

## LIST OF FIGURES

Figure 1	Hydrolytic behavior of chlorethoxyfos (CE) over the pH range of 3-11. Insert: slope represents the alkaline hydrolysis rate coefficient. $[CE]_0 = 0.5 \mu\text{M}$ , $[\text{Buffer}]_T = 10 \text{ mM}$ , and Temperature = $25 \pm 1^\circ\text{C}$ . Error bars represent 95% confidence intervals....	40
Figure 2	Hydrolytic behavior of tebupirimfos (TE) over the pH range of 3-10. Insert: slope represents the alkaline hydrolysis rate coefficient. $[TE]_0 = 0.5 \mu\text{M}$ , $[\text{Buffer}]_T = 10 \text{ mM}$ , and Temperature = $25 \pm 1^\circ\text{C}$ . Error bars represent 95% confidence intervals....	41
Figure 3	Hydrolytic behavior of methidathion (ME) over the pH range of 3-11. Insert: slope represents the alkaline hydrolysis rate coefficient. $[ME]_0 = 0.5 \mu\text{M}$ , $[\text{Buffer}]_T = 10 \text{ mM}$ , and Temperature = $25 \pm 1^\circ\text{C}$ . Error bars represent 95% confidence intervals....	42
Figure 4	Hydrolytic behavior of phosmet (PM) over the pH range of 2-10. Insert: slope represents the alkaline hydrolysis rate coefficient. $[PM]_0 = 0.5 \mu\text{M}$ , $[\text{Buffer}]_T = 10 \text{ mM}$ , and Temperature = $25 \pm 1^\circ\text{C}$ . Error bars represent 95% confidence intervals....	43
Figure 5	Observed first-order rate of CE loss in the presence of aqueous chlorine at pH 6.5. $[CE]_0 = 0.5 \mu\text{M}$ , $[\text{HOCl}]_0 = 10\text{-}100 \mu\text{M}$ , $[\text{PO}_4]_T = 10 \text{ mM}$ , and Temperature = $25 \pm 1^\circ\text{C}$ . Experiments performed in triplicate.....	44
Figure 6	Observed first-order rate of DZ loss in the presence of aqueous chlorine at pH 6.5. $[DZ]_0 = 0.5 \mu\text{M}$ , $[\text{HOCl}]_0 = 10\text{-}100 \mu\text{M}$ , $[\text{PO}_4]_T = 10 \text{ mM}$ , and Temperature = $25 \pm 1^\circ\text{C}$ . Experiments performed in triplicate.....	45
Figure 7	Observed first-order rate of MA loss in the presence of aqueous chlorine at pH 6.5. $[\text{MA}]_0 = 0.5 \mu\text{M}$ , $[\text{HOCl}]_0 = 10\text{-}100 \mu\text{M}$ , $[\text{PO}_4]_T = 10 \text{ mM}$ , and Temperature = $25 \pm 1^\circ\text{C}$ . Experiments performed in triplicate.....	46
Figure 8	Observed first-order rate of ME loss in the presence of aqueous chlorine at pH 6.5. $[\text{ME}]_0 = 0.5 \mu\text{M}$ , $[\text{HOCl}]_0 = 10\text{-}100 \mu\text{M}$ , $[\text{PO}_4]_T = 10 \text{ mM}$ , and Temperature = $25 \pm 1^\circ\text{C}$ . Experiments performed in triplicate.....	47
Figure 9	Observed first-order rate of PA loss in the presence of aqueous chlorine at pH 6.5. $[\text{PA}]_0 = 0.5 \mu\text{M}$ , $[\text{HOCl}]_0 = 10\text{-}100 \mu\text{M}$ , $[\text{PO}_4]_T = 10 \text{ mM}$ , and Temperature = $25 \pm 1^\circ\text{C}$ . Experiments performed in triplicate.....	48
Figure 10	Observed first-order rate of PM loss in the presence of aqueous chlorine at pH 6.5. $[\text{PM}]_0 = 0.5 \mu\text{M}$ , $[\text{HOCl}]_0 = 10\text{-}100 \mu\text{M}$ , $[\text{PO}_4]_T = 10 \text{ mM}$ , and Temperature = $25 \pm 1^\circ\text{C}$ . Experiments performed in triplicate.....	49
Figure 11	Observed first-order rate of TE loss in the presence of aqueous chlorine at pH 6.5. $[\text{TE}]_0 = 0.5 \mu\text{M}$ , $[\text{HOCl}]_0 = 10\text{-}100 \mu\text{M}$ , $[\text{PO}_4]_T = 10 \text{ mM}$ , and Temperature = $25 \pm 1^\circ\text{C}$ . Experiments performed in triplicate.....	50



Figure 12	The reaction order of chlorine with 8 OP pesticides at pH 6.5. $[\text{OP}]_0 = 0.5 \mu\text{M}$ , $[\text{PO}_4]_{\text{T}} = 10 \text{ mM}$ , Temperature = $25 \pm 1^\circ\text{C}$ , and $[\text{HOCl}]_{\text{T}} = 10\text{-}100 \mu\text{M}$ .....	51
Figure 13	Second-order apparent rate coefficient for the OP pesticides at pH 6.5. $[\text{OP}]_0 = 0.5 \mu\text{M}$ , $[\text{PO}_4]_{\text{T}} = 10 \text{ mM}$ , Temperature = $25 \pm 1^\circ\text{C}$ , and $[\text{HOCl}]_{\text{T}} = 0\text{-}100 \mu\text{M}$ . Error bars represent 95% confidence intervals. ....	52
Figure 14	The pH dependency of the first-order observed rate coefficients for the OP pesticides. $[\text{OP}]_0 = 0.5 \mu\text{M}$ , $[\text{HOCl}]_{\text{T}} = 25 \mu\text{M}$ , $[\text{Buffer}]_{\text{T}} = 10 \text{ mM}$ , and Temperature = $25^\circ\text{C}$ . Error bars represent 95% confidence intervals. ....	53
Figure 15	Second-order apparent rate coefficient for the OP pesticides at pH 9. $[\text{OP}]_0 = 0.5 \mu\text{M}$ , $[\text{CO}_3]_{\text{T}} = 10 \text{ mM}$ , Temperature = $25 \pm 1^\circ\text{C}$ , and $[\text{HOCl}]_{\text{T}} = 0\text{-}100 \mu\text{M}$ . Error bars represent 95% confidence intervals. ....	54
Figure 16	Relationship between the $k_{\text{HOCl,OP}}$ with $E_{\text{HOMO}}$ as a function of OP pesticide subgroup. Error bars about the regression line represent 95% confidence intervals. ....	55
Figure 17	Relationship between the $k_{\text{OCl,OP}}$ with alkaline hydrolysis rate coefficient as a function of OP pesticide subgroup. Error bars about the regression line represent 95% confidence intervals. ....	56
Figure 18	Second-order apparent rate coefficient of 3 OP pesticide oxons at pH 9. $[\text{OP}]_0 = 0.5 \mu\text{M}$ , $[\text{CO}_3]_{\text{T}} = 10 \text{ mM}$ , Temperature = $25 \pm 1^\circ\text{C}$ , and $[\text{HOCl}]_{\text{T}} = 0\text{-}200 \mu\text{M}$ . Error bars represent 95% confidence intervals for both data points and regression lines. ....	57
Figure 19	Experimental and model results for DZ loss in the presence of chlorine at pH 7.0. $[\text{DZ}]_0 = 0.6 \mu\text{M}$ , $[\text{HOCl}]_{\text{T}} = 20 \mu\text{M}$ , $[\text{PO}_4]_{\text{T}} = 10 \text{ mM}$ , and Temperature = $25 \pm 1^\circ\text{C}$ . Error bars represent 95% confidence intervals. Lines represent model results. ....	58
Figure 20	Experimental and model results for PA loss in the presence of chlorine at pH 8.0. $[\text{PA}]_0 = 0.57 \mu\text{M}$ , $[\text{HOCl}]_{\text{T}} = 25 \mu\text{M}$ , $[\text{PO}_4]_{\text{T}} = 10 \text{ mM}$ , and Temperature = $25 \pm 1^\circ\text{C}$ . Lines represent model results.....	59
Figure 21	First-order observed loss of CP and DZ in the presence of monochloramine as a function of pH. $[\text{NH}_2\text{Cl}] = 50 \mu\text{M}$ , $[\text{OP}]_0 = 0.5 \mu\text{M}$ , $\text{Cl/N} = 0.7 \text{ mol/mol}$ , $[\text{Buffer}]_{\text{T}} = 10 \text{ mM}$ , Temperature = $25 \pm 1^\circ\text{C}$ , and pH 6.5-9.0. Error bars represent 95% confidence intervals. ....	60
Figure 22	First-order observed loss of MA in the presence of monochloramine as a function of pH. $[\text{NH}_2\text{Cl}] = 50 \mu\text{M}$ , $[\text{MA}]_0 = 0.5 \mu\text{M}$ , $\text{Cl/N} = 0.7 \text{ mol/mol}$ , $[\text{Buffer}]_{\text{T}} = 10 \text{ mM}$ , Temperature = $25 \pm 1^\circ\text{C}$ , and pH 6.5-9.0. Error bars represent 95% confidence intervals.....	61

Figure 23	Observed first-order observed loss of three OP pesticides in the presence of monochloramine at pH 8.5. $[\text{NH}_2\text{Cl}] = 50 \mu\text{M}$ , $[\text{OP}]_0 = 0.5 \mu\text{M}$ , $\text{Cl/N} = 0\text{-}0.7 \text{ mol/mol}$ , $[\text{H}_3\text{BO}_3]_{\text{T}} = 10 \text{ mM}$ , and Temperature = $25 \pm 1^\circ\text{C}$ . Error bars represent 95% confidence intervals. ....	62
Figure 24	Experimental and model results for CP loss in the presence of monochloramine. $[\text{CP}]_0 = 0.5 \mu\text{M}$ , $[\text{NH}_2\text{Cl}]_0 = 50 \mu\text{M}$ , $\text{Cl/N} = 0.7 \text{ mol/mol}$ , $[\text{Buffer}]_{\text{T}} = 10 \text{ mM}$ , pH 6.5-9, and Temperature = $25 \pm 1^\circ\text{C}$ . Error bars represent 95% confidence intervals. Lines represent model results. ....	63
Figure 25	Experimental and model results for DZ loss in the presence of monochloramine. $[\text{DZ}]_0 = 0.5 \mu\text{M}$ , $[\text{NH}_2\text{Cl}]_0 = 50 \mu\text{M}$ , $\text{Cl/N} = 0.7 \text{ mol/mol}$ , $[\text{Buffer}]_{\text{T}} = 10 \text{ mM}$ , pH 6.5-9, and Temperature = $25 \pm 1^\circ\text{C}$ . Error bars represent 95% confidence intervals. Lines represent model results. ....	64
Figure 26	Experimental and model results for MA loss in the presence of monochloramine. $[\text{MA}]_0 = 0.5 \mu\text{M}$ , $[\text{NH}_2\text{Cl}]_0 = 50 \mu\text{M}$ , $\text{Cl/N} = 0.7 \text{ mol/mol}$ , $[\text{Buffer}]_{\text{T}} = 10 \text{ mM}$ , pH 6.5-8.5, and Temperature = $25 \pm 1^\circ\text{C}$ . Error bars represent 95% confidence intervals. Lines represent model results.....	65
Figure 27	Structure-activity relationship relating the reaction of monochloramine, dichloramine, and hypochlorous acid with CP, DZ, and MA. Piela and Wrona (49) found half-wave potentials for monochloramine (-0.2 V), dichloramine (0.4), and hypochlorous acid (0.8 V). These values were then converted using the Nernst equation to the intensive property of the log ratio of the activities of the reduced products to the oxidized forms of the oxidant. ....	66

## EXECUTIVE SUMMARY

Environmental regulations require that all relevant routes of human exposure to anthropogenic chemicals be considered in risk assessments. Community water systems (CWSs) serve approximately 95% of the US population and potable water is considered a relevant route of exposure to anthropogenic chemicals. There is available monitoring data for high priority pesticides and toxic chemicals in drinking water sources (both surface and ground water). However, there is very little monitoring data for these chemicals or their transformation products in finished drinking water. Limited experimental studies show that some chemicals are partially removed by physical water treatment processes (e.g., filtration, flocculation, etc.), and some are transformed by reactions that occur during chemical treatment (e.g., disinfection and softening). Transformation products of some contaminants have been shown to be more toxic than the parent compound.

This report is in partial fulfillment of the National Exposure Research Laboratory Task # ERD08103-1, “Fate of Pesticides and Toxic Chemicals During Drinking Water Treatment”, under Safe Pesticides/Safe Products (SP2) Long-Term Goal 1.4.1. The goals of this research task are to: 1) provide chemical-specific information on the effects of water treatment for high-priority pollutants, 2) provide physicochemical parameters for transformation products, and 3) develop predictive models for forecasting treatment effects that cross chemical class and treatment conditions.

The work reported here demonstrates a “proof-of-concept” towards the development of a comprehensive modeling tool for OP pesticide fate in drinking water treatment plants and distribution systems. Our objective was to develop predictive models that associate intrinsic rates of reactivity to structural variability. This will allow decision makers to rank and prioritize chemicals found in drinking water sources according to potential risk. For this purpose, eight OP

pesticides and three oxon transformation products were investigated. The 8 OP pesticides chosen for this study contained the thiophosphate moiety ( $P=S$ ) from the phosphorothioate (chlorethoxyfos (CE), chlorpyrifos (CP), diazinon (DZ), parathion (PA), and tebupirimfos (TE)) and the phosphorodithioate (malathion (MA), methidathion (ME), and phosmet (PM)) subgroups. The three oxon (i.e.,  $P=O$ ) products were from the phosphate subgroup (diazoxon (DZO), malaoxon (MAO), and paraoxon (PAO)). It was originally thought that by investigating a class of pesticides that structure-activity relationships could easily be developed. However, reactivity with chlorinated oxidants could only be correlated with subgroups and not across the class of OP pesticides.

The phosphorodithioate subgroup was found to hydrolyze much more rapidly than the phosphate or the phosphorothioate subgroups, and oxons are more susceptible to alkaline hydrolysis when compared to the corresponding thionates. Also, ethyl esters appear to hinder nucleophilic attack by hydroxide ions (i.e., alkaline hydrolysis) compared to a structurally similar pesticide with methyl ester linkages at the phosphorus atom; however, there is a need for more hydrolysis studies to be conducted at environmentally relevant conditions to build structure-activity relationships in order to predict intrinsic hydrolysis rate coefficients.

In the presence of chlorine, intrinsic rate coefficients for both hypochlorous acid ( $HOCl$ ) and hypochlorite ( $OCl^-$ ) were calculated,  $k_{HOCl,OP}$  and  $k_{OCl,OP}$  respectively. Since multiple reaction pathways occur simultaneously over the pH range of 6.5-9, a chlorine-OP pesticide reaction model previously developed for CP was used. The reaction with  $HOCl$  and the OP pesticides resulted in the rapid formation of oxons, which are more toxic than the parent OP pesticide. Hypochlorite accelerated the hydrolysis of each OP pesticide but did not result in oxon formation. The energy of the highest occupied molecular orbital ( $E_{HOMO}$ ) showed that

$k_{\text{HOCl,OP}}$  correlated within the two subgroups. The alkaline hydrolysis rate ( $k_{\text{B,OP}}$ ) was found to correlate with  $k_{\text{OCl,OP}}$  within each OP subgroup, which also implies that the reaction mechanism of  $\text{OCl}^-$  and  $\text{OH}^-$  are similar. Therefore, the cross correlation demonstrates that  $\text{OCl}^-$  does act as a nucleophile accelerating the hydrolysis of OP pesticides. Oxons did not undergo further oxidation by aqueous chlorine, but they were susceptible to chlorine assisted hydrolysis.

Three of the most commonly detected OP pesticides (CP, DZ, and MA) in drinking water supplies were investigated in the presence of chloramines. The loss of all three pesticides under chloramination conditions was found to be highly pH dependent. At pH 6.5, the primary degradation pathway for OP pesticides was due to reaction with dichloramine and hypochlorous acid, which are formed during monochloramine autodecomposition. The direct reaction of monochloramine with each OP pesticide was found to be a minimal loss pathway. The order of reactivity for the three chlorinated oxidants was  $\text{HOCl} \gg \text{NHCl}_2 \gg \text{NH}_2\text{Cl}$ . The reactivity of the three chlorinated oxidants was found to correlate with half-wave potentials ( $E_{1/2}$ ) for each OP pesticide.

The stability of OP pesticides was investigated under conditions similar to drinking water treatment. The critical reaction parameters could not be correlated across the OP pesticide class, but correlations were made within subgroups indicating that minute structure differences significantly impact reactivity. The structure-activity relationships developed here could allow for the prediction of critical reaction parameters of OP pesticides in the presence of chlorinated oxidants. Along with the presented model, regulators could assess the potential risk associated when consuming potable water contaminated with OP pesticides.

## **1 INTRODUCTION**

The United States Geological Survey (USGS) conducts a national reconnaissance survey known as NAWQA (National Water-Quality Assessment) Program to help define the effect contaminants have on drinking water supplies and aquatic ecosystems (1). 90 pesticides and some selected metabolites were chosen as target chemicals to monitor in US drinking water sources. However, there is a relative dearth of information on occurrence of pesticide residuals and pesticide metabolites in finished drinking water. Two surveys have been conducted for a few community water systems examining pesticide concentrations in the source and finished drinking water (2, 3). Neither of these studies thoroughly examined the effect of each treatment process on a single slug of water, hence only the influent and effluent of each treatment facility could be qualitatively discussed with respect to overall removal efficacy. Also, these studies did not account for the treatment plant hydraulic retention time, thus it was not possible to ensure that influent and effluent samples were properly paired.

The Food Quality Protection Act of 1996 (FQPA) requires that all pesticide chemical residuals in or on food be considered for anticipated human exposure. Drinking water is considered a potential pathway for dietary exposure, but there is reliable monitoring data for only the source water. When assessing potential pesticide exposure due to drinking potable water, all potential transformation pathways need to be addressed. Under drinking water treatment conditions, hydrolysis and chemical oxidation are the most relevant transformation pathways for the class of organophosphorus (OP) pesticides (4). The OP pesticides were chosen for their wide-spread use and measured concentrations in drinking water supplies (1, 3, 5). However, there is little quantitative rate coefficient information for either pathway.

Only 6 OP pesticides have been studied in-depth to reveal their hydrolytic behavior at acidic, neutral, or alkaline conditions. Malathion has been extensively studied over the pH range

of 1-10. In the pH range of 1-4, hydrolysis occurs at an ether linkage resulting in the formation of malathion monoacid (6). Above pH of 4, nucleophilic attack at the tetrahedral phosphorus atom by hydroxide ion was found to be twice as fast as carboxyl ester hydrolysis (7). Malathion appears to be the most stable at pH 4, with an estimated half-life greater than one year.

Diazinon, diazoxon, parathion, and paraoxon have been studied over the pH range of 3.1-10.4 (8). All four of these OP pesticides were found to have an acidic, neutral, and alkaline component to their hydrolytic behavior. Also, chlorpyrifos and its corresponding oxon were studied over the pH range of 3-11, which neutral and alkaline hydrolysis rate coefficients were determined for both pesticides (4, 9). However, OP pesticide hydrolysis is very dependent on structure allowing for rate coefficient comparisons only to be made within each subgroup (i.e., phosphorothioate, phosphorodithioate, phosphorothiolate, and phosphate) (8).

Chlorination is the most commonly used chemical disinfection process for community water systems (10), and it is known to react with numerous pesticides. For example, four s-triazines were found to degrade in the presence of aqueous chlorine ( $[\text{HOCl}]_{\text{T}} = \text{HOCl} + \text{OCl}^-$ ) (11, 12). Atrazine was also found to be significantly degraded by ozone (13); however, subsequent chlorination of the ozonated effluent had very little effect on the concentration of residual atrazine or its ozone degradation products (2). Also, some carbamate pesticides have been shown to react with chlorine while other members of this pesticide class were found to be stable in chlorinated water. For example, carbaryl and propoxur do not react with chlorine; but aldicarb, methomyl, and thiobencarb do exhibit significant reactivity (14-16). These findings demonstrate that chlorine reactivity with different members in a specific class of pesticides can vary significantly due to chemical structure variations. Therefore, it is prudent to study the fate and transformation pathways of entire chemical classes, using class members that exhibit

systematic structural variations and employing carefully selected experimentation and numerical modeling.

When chlorine reacts with the phosphorothioate subgroup of organophosphorus (OP) pesticides, the thiophosphate functionality ( $\text{P}=\text{S}$ ) can be oxidized to its corresponding oxon ( $\text{P}=\text{O}$ ) (17-19). The resulting oxons are typically more potent than the parent as an inhibitor of acetylcholinesterase, an enzyme necessary for regulating nerve impulse transmission between nerve fibers (19). Duirk and Collette, (4) elucidated the fate of chlorpyrifos (CP) and its transformation products over the pH range of 6-11. They were able to model the loss of CP and chlorpyrifos oxon (CPO) to the stable end-product of 3,5,6-trichloro-2-pyridinol (TCP) over this pH range in buffered deionized water systems, as well as in the presence of naturally occurring aqueous constituents such as bromide and natural organic matter (NOM) (20).

Chloramines are a common secondary disinfectant alternative for many drinking water utilities. In some cases, monochloramine is used for both primary and secondary disinfection when excessively high background ammonia concentration in the source water do not allow for breakpoint chlorination (10). However, very little is known about the reactions of monochloramine with anthropogenic chemicals. In the presence of aromatic-ether and amine-containing pharmaceuticals, aqueous chlorine was found to react more rapidly than monochloramine (21). Also, monochloramine was found to react with diuron, a phenyl urea herbicide, resulting in the formation of N-nitrosodimethylamine (NDMA) (22), which is a known disinfection byproduct of chloramination (22, 23).

However, it is difficult to directly observe monochloramine reactions with anthropogenic compounds due to its own autodecomposition, i.e., a series of reactions ultimately resulting in monochloramine loss (Table 1) (24). This mechanism is highly pH dependent and allows for



multiple oxidants to coexist (i.e., monochloramine ( $\text{NH}_2\text{Cl}$ ), dichloramine ( $\text{NHCl}_2$ ), and  $\text{HOCl}$ ), which confounds the interpretation of observational results. Using this well understood autodecomposition reaction mechanism, the reactions of monochloramine with natural organic matter resulting in chlorinated and brominated disinfection byproduct formation (DBP) were resolved (25-27). This same technique has been used to investigate triclosan reactivity in chloraminated water (28). It was found that dichloramine was approximately three orders of magnitude more reactive with triclosan than monochloramine, but aqueous chlorine was found to be three orders of magnitude faster than dichloramine. Similar results have been seen with sulfite and cyanide (29). Therefore, reaction pathway models can be used as a tool to propose and elucidate reaction pathways in complex systems with parallel reactions.

The purpose of this study was to further elucidate the kinetics and transformation pathways of OP pesticides in the presence of chlorinated oxidants. The 8 OP pesticides chosen in this study contained the thiophosphate moiety from the phosphorothioate (chloroethoxyfos (CE), chlorpyrifos (CP), diazinon (DZ), parathion (PA), and tebupirimfos (TE)) and the phosphorothioate (malathion (MA), methidathion (ME), and phosmet (PM)) subgroups (Table 2). Hydrolysis neutral and alkaline rate coefficients were determined for CE, ME, PM, and TE. Since all these OP pesticides can form oxons in the presence of chlorine, reaction rate coefficients  $\text{HOCl}$  and  $\text{OCl}^-$  were correlated to molecular descriptors. For both correlations, subgroup differences were observed. CP, DZ, and MA were investigated in the presence of monochloramine over the pH range of 6.5-9. These three OP pesticides were chosen due to their frequency of detection in drinking water supplies (3).

## 2 EXPERIMENTAL PROCEDURES

### 2.1 *Materials*

Chlorpyrifos (CP), chlorpyrifos oxon (CPO), 3,5,6-trichloro-2-pyridinol (TCP), parathion (PA), paraoxon (PAO), 4-nitrophenol (n-Ph), diazinon (DZ), diazoxon (DZO), 2-isopropyl-6-methyl-4-pyrimidinol (IMP), malathion (MA), malaoxon (MAO), methidathion (ME), tebupirimfos (TE), phosmet (PM) and chlorethoxyfos (CE) were purchased from ChemService (West Chester, PA). Commercial 10-13% sodium hypochlorite (NaOCl), purchased from Aldrich (Milwaukee, WI), contained equal-molar amounts of  $\text{OCl}^-$  and  $\text{Cl}^-$ . Aqueous stock solutions and experiments utilized laboratory prepared deionized water ( $18 \text{ M}\Omega \text{ cm}^{-1}$ ) from a Barnstead ROPure Infinity™/NANOPure™ system (Barnstead-Thermolyne Corp., Dubuque, IA). Filters with pore size of  $0.45 \mu\text{m}$  were purchased from Millipore (Billerica, MA). Phosphate and carbonate salts used for buffer solutions were dissolved in deionized water and filtered through a  $0.45 \mu\text{m}$  filter, which was pre-rinsed with deionized water. The pH for the experiments was adjusted with either 1 N  $\text{H}_2\text{SO}_4$  or NaOH. All other organic and inorganic chemicals were certified ACS reagent grade and used without further purification. The glassware and polytetrafluoroethylene (PTFE) septa used in this study were soaked in a concentrated free chlorine solution for 24 hours, rinsed with deionized water, and dried prior to use. All chlorination, hydrolysis, and chloramination experiments were conducted at constant temperature ( $25 \pm 1^\circ\text{C}$ ) and pH was maintained to  $\pm 0.1$  of the initial pH for the duration of each experiment.

### 2.2 *Methods*

#### 2.2.1 *Chlorination and Hydrolysis of OP Pesticides*

For all OP oxidation and hydrolysis experiments, each OP was spiked by adding 1 mL of 4 mM stock in ethyl acetate into an empty 4 L borosilicate glass Erlenmeyer flask. A gentle flow

of nitrogen gas was used to evaporate the ethyl acetate and 4 L of deionized water was then added to the flask. The solution was slowly stirred and allowed to dissolve for 12 hours resulting in an aqueous OP concentration of 1  $\mu\text{M}$ .

OP chlorination kinetic experiments were conducted under pseudo first-order conditions: total chlorine,  $[\text{HOCl}]_{\text{T}}$ , to OP molar ratios of 20:1, 50:1, 100:1, and 200:1. Chlorine was added to solutions under rapid mix conditions achieved with a magnetic stir plate and a PTFE coated stir bar. All chlorination experiments were conducted until at least 87% loss in the pesticide initial concentration was achieved. Above pH 8, 10 mM carbonate  $[\text{CO}_3]_{\text{T}}$  buffer was used to maintain pH. The commercial aqueous chlorine solution was first diluted to 250 mM and then added to the aqueous system containing 0.5  $\mu\text{M}$  OP pesticide and carbonate buffer in a 2 L Erlenmeyer flask. Thirteen aliquots from the large 2 L reactor were then placed into 120 mL amber reaction vessels with PTFE septa and stored in the dark. In the pH range of 6.5-8, the rate of OP loss in the presence of chlorine was very fast. Therefore, thirteen 100 mL aliquots of the 2 L aqueous system containing 10 mM phosphate buffer,  $[\text{PO}_4]_{\text{T}}$ , and 0.5  $\mu\text{M}$  OP were placed in 250 mL amber Erlenmeyer flasks. Each flask was individually dosed with chlorine.

At each discrete sampling interval, two reaction vessels were sacrificed in their entirety. One vessel was used to determine total chlorine concentration ( $[\text{HOCl}]_{\text{T}} = [\text{HOCl}] + [\text{OCl}^-]$ ) via Standard Method 4500-Cl F DPD-FAS titrimetric method (30). Free chlorine residuals were quenched in the second reaction vessel with sodium sulfite in 20% excess of the initial free chlorine concentration and the pH of the 100 mL sample was then adjusted to 7. Sulfite had no effect on the recovery of any of the analytes as previously shown (4).

Hydrolysis experiments were conducted in a similar manner to the chlorination experiments. Phosphate buffer was used over the pH range of 2-8; while carbonate buffer was

used in the experiments at alkaline pH. Since hydrolysis of most of the OP pesticides was relatively slow, these experiments were conducted in 2-L Erlenmeyer flasks with 10 mM of buffer. However, the hydrolysis rate of PM was extremely fast at pH 9-10. The experimental setup used to study the chlorination of OP pesticides at neutral pH was modified in order to study PM hydrolysis at alkaline pH. Instead of spiking a 100 mL solution under rapid mix conditions with a minuscule amount of chlorine, 98 mL of a  $[PM]_0 = 0.5 \mu\text{M}$  solution was spiked with 2 mL of concentrated carbonate buffer. The concentrated buffer solution was the proper proportion of bicarbonate/carbonate, which immediately adjusted the 100 mL sample to the target pH of 9, 9.5, or 10. The rapid rate of PM hydrolysis at alkaline pH was then stopped by immediately adjusting the pH to 7 with the appropriate amount of sulfuric acid. Hydrolysis experiments were conducted until at least 70% loss in the initial pesticide concentration was achieved.

### 2.2.2 Chloramination of OP Pesticides

Monochloramine kinetic experiments utilized additions of preformed monochloramine to avoid potential artifacts caused by reactions of excess free chlorine that may briefly exist if monochloramine was formed in-situ. The stock solution was prepared by mixing 5.64 mM ammonia with 3.7 mM hypochlorous acid to achieve the desired 0.7 Cl/N molar ratio. The solution was aged for 30 minutes in 10 mM bicarbonate buffer, pH 8.5, prior to use in any of the experiments. Kinetic experiments were performed in a 2 liter Erlenmeyer flask in which monochloramine ( $[\text{NH}_2\text{Cl}]_0 = 0.05 \text{ mM}$ ) was added to a buffer ( $[\text{Buffer}]_T = 10.0 \text{ mM}$ ) solution containing  $[\text{OP}]_0 = 0.5 \mu\text{M}$  under rapid mix conditions, which was then poured into sixteen 128 mL batch reactors. At each sample interval, two reactors were used in their entirety and monochloramine, pH, as well as the pesticide and its known degradation products were measured for at least 140 hours.

### **2.3 *OP Pesticide Analysis***

Parent OP, oxon products, and other degradation products were extracted using C-18 solid phase extraction cartridges purchased from Supleco (Bellefonte, PA). Prior to extraction, the sample was spiked with 1  $\mu$ M of phenthorate (internal standard), mixed thoroughly by hand for two minutes, passed through the SPE cartridge at an approximate flow-rate of 7 mL/min, and eluted with 3 mL of ethyl acetate. Quantification for each analyte was compared to eight extracted standards over the concentration range of 0.01 to 1  $\mu$ M. A Hewlett-Packard 6890 GC equipped with a 5973 MSD was used to analyze the OPs and their degradation products. GC conditions were as follows: 30-m Restek Rtx-200 column with a 0.25-mm ID and 0.5- $\mu$ m film thickness. The temperature profile was: 100°C for 5 minutes, 100 to 250°C at 10 °C/minute, and then held at 250°C for 25 minutes.

### **2.4 *Numerical Calculations and Parameter Estimation***

Scientist™ by Micromath (Salt Lake City, UT) was used to solve the systems of stiff ordinary differential equations. The model was used to estimate rate coefficients using non-linear regression analysis techniques. Scientist uses a modified Powell algorithm to minimize the unweighted sum of the squares of the residual error between the predicted and experimentally observed values to estimate specific parameters in the model. Final parameter estimates were based on global pooling of all experimental data for each OP pesticide. All molecular descriptors were calculated using GAMESSPLUS software.

### 3 RESULTS AND DISCUSSION

#### 3.1 *Hydrolysis of select OP pesticides*

Understanding the hydrolytic behavior of water soluble pesticides, such as the OP pesticides, is paramount in order to determine their fate in the environment or engineered systems. The phosphorothioate subgroup examined contained five pesticides. Of these, very little information was known about CE or TE. CE was first investigated at pH 3 and 7 in order to determine the acidic and neutral hydrolysis rate coefficients. The hydrolytic behavior was similar to CP over this pH range and CE exhibited no statistical difference in the first order observed rate coefficient at pH 3 or 7 (Figure 1). At alkaline pH, hydroxide ion appears to significantly accelerate CE hydrolysis (Figure 1, insert). TE was also investigated over the pH range of 3-10 with only slightly different results (Figure 2). At pH 3 and 7, the observed first-order rate coefficients of TE hydrolysis were statistically similar. However, the observed rate of TE loss at pH 10 was found to be statistically larger than the observed rate at either pH 3 or 7. The presence of hydroxide ion at pH 10 appears to slightly increase the observed rate of TE loss. Since the observed hydrolysis rate of TE at pH 7 was only minimally different when compared to the observed hydrolysis rate at pH 10, the second order alkaline hydrolysis rate coefficient was estimated from these two pHs (Figure 2, insert).

The neutral hydrolysis rates for both TE and CE were found to be very similar with CP, DZ, and PA. Neutral hydrolysis rates for the phosphorothioate subgroup ranged from  $1.56 \times 10^{-4}$  –  $1.10 \times 10^{-3} \text{ h}^{-1}$ . However, the range in second-order rate coefficients for alkaline hydrolysis was significantly greater but with most of the OP pesticides relatively close in magnitude (Table 3). CP, DZ, PA, and TE second order hydrolysis rate coefficients ranged from  $6.0$ - $37.1 \text{ M}^{-1} \text{ h}^{-1}$ . However, CE was found to be 2 orders of magnitude faster than CP. Hydroxide ion attacks the tetrahedral phosphorus atom via an  $\text{S}_{\text{N}}2$  nucleophilic substitution releasing the best leaving group

and resulting in the formation of diethyl thiophosphate. CP, DZ, PA, and TE all have aryl functional groups as leaving groups. CE has an alkyl leaving group with four chlorine atoms. The highly electronegative chlorine atoms may draw the electrons associated with the phospho-ether linkage creating a slightly more partial positive charge at the tetrahedral phosphorous atom, which would allow CE to be more susceptible to  $S_N2$  attack by hydroxide ion. CP also has chlorine atoms associated with the aryl structure and is more susceptible to nucleophilic attack than the other phosphorothioates; however, the aryl structure appears to significantly negate the electron withdrawing effects of the three chlorine atoms. The oxons of DZ, PA, and CP (i.e., phosphate subgroup) have all previously been examined (4, 8). The alkaline hydrolysis rate for the oxons in the phosphate subgroup is an order of magnitude faster than their corresponding phosphorothioates (Table 3), which has been previously reported (4, 8, 31). This demonstrates that the alkaline hydrolysis rate of OP pesticides can be significantly different with minor changes in molecular structure.

In the phosphorodithioate subgroup, MA was the only pesticide in this subgroup in which its hydrolytic behavior has been well characterized (6, 7). The observed rate coefficients for ME at pH 3 and 7 were statistically indistinguishable (Figure 3). At pH 10 and above, ME alkaline hydrolysis was very rapid (Figure 3, insert). PM was found to be relatively stable at pH 2; however, its hydrolysis increased rapidly with increasing hydroxide ion concentration (Figure 4). Alkaline hydrolysis of PM was found to be very rapid above pH 8 (Figure 4, insert). For the phosphorodithioate subgroup, ME was the only OP pesticide in this subgroup found to be stable at neutral pH. Neutral hydrolysis for the phosphorodithioate subgroup was then operationally defined as the pH where each pesticide was the most stable. By this definition, the neutral hydrolysis rate coefficients are comparable to the phosphorothioate and phosphate subgroups.

Alkaline hydrolysis was generally found to be more rapid than the other two subgroups. All the phosphorodithioate pesticides in Table 2 have methyl esters linkages at the tetrahedral phosphorus atom. Alkaline hydrolysis may be faster due to the fact that S<sub>N</sub>2 nucleophilic attack by the hydroxide ion is hindered more by the ethyl esters than the methyl esters. Chlorpyrifos and parathion alkaline hydrolysis rates have been found to be slower when compared to chlorpyrifos-methyl and parathion-methyl (8). Also, the thiol ester could be more susceptible to nucleophilic attack by hydroxide ion than phenyl esters. This makes it difficult to directly compare the phosphorodithioates to the phosphorothioates at environmentally relevant conditions.

### 3.2 *OP Pesticide Degradation in the Presence of Aqueous Chlorine*

In the presence of aqueous chlorine, the oxidation of CP was found to be first order resulting in an overall second order reaction (4). Therefore, observed loss of each OP pesticide in the presence of aqueous chlorine was assumed to be first order with respect to the OP pesticide. If  $\ln([OP]/[OP]_0)$  versus time (t) plots are linear, then this assumption would be valid when there is a molar excess of chlorine. The observed first-order rate coefficients ( $k_{obs}$ ) for all the OP pesticides were determined from these plots via the slope of the regression line as shown in the following expression.

$$\ln \frac{[OP]}{[OP]_0} = -k_{obs} t \quad (1)$$

Under pseudo first-order chlorination conditions, all the OP pesticides from CE-TE exhibited a first order dependency with respect to the OP pesticide in the presence of excess aqueous chlorine at pH 6.5 (Figures 5-11). The reaction order of the aqueous chlorine reacting with each OP pesticide was determined by plotting the log of  $k_{obs}$  versus the log of the initial chlorine



concentration at pH 6.5 (Figure 12). Since the slope of the regression line is approximately 1 for all OPs, this indicates that the loss of OP pesticides can be described as a second-order reaction.

The apparent loss of each OP pesticide in the presence of aqueous chlorine at a specific pH could then be described by the following rate expression where  $k_{app}$  is the apparent second-order rate coefficient at a specific pH (equation 2). The observed first-order rate coefficients at

$$\frac{d[OP]}{dt} = -k_{app}[HOCl]_T[OP] \quad (2)$$

each pH were assumed to linearly increase with increasing free chlorine concentration (equation 3). The  $k_{app}$  for each OP pesticide was determined by plotting  $k_{obs}$  versus the initial

$$k_{obs} = k_{app}[HOCl]_T \quad (3)$$

total aqueous chlorine concentration. Figure 13 shows that  $k_{obs}$  increased linearly with increasing chlorine concentration at pH of 6.5. Diazinon and phosmet degraded the fastest at this pH, while the rest of the OP pesticides exhibited similar reactivity with aqueous chlorine. Since approximately 91% of the active chlorine is in the HOCl form, the apparent rate coefficient will be very close to the intrinsic rate coefficient of hypochlorous acid reacting with each OP pesticide. As pH increased from 6.5 to 9,  $k_{obs}$  decreased for all the OP pesticides (Figure 14).

When the pH of the aqueous system shifts from neutral to alkaline pH, the chlorine species also shifts from HOCl, which has a  $pK_a$  of 7.5 (32), to  $OCl^-$ . The decrease in the  $k_{obs}$  would be expected if hypochlorous acid is the dominant reacting species resulting in oxon formation.

Oxons for all the parent OP pesticides are not commercially available; therefore, transformation products were identified by their mass spectra. For all the OP pesticides, their corresponding oxons were the only transformation products identified by NIST mass spectra database at pH 6.5. HOCl appears to be the active chlorine species over the pH range investigated responsible for OP oxidation and oxon formation.

The transformation of OP pesticides can become relatively complicated at alkaline pH. Several transformation pathways occur simultaneously resulting in unique transformation products for each pathway. At pH 9, approximately 97% of the active chlorine will be in the hypochlorite form. However, all the OP pesticides degraded rapidly in the presence of aqueous chlorine (Figure 15). Phosmet degraded faster than diazinon due to PM being more susceptible to alkaline hydrolysis. Just like at pH 6.5, the observed rate coefficients increased linearly with increasing chlorine concentration. However, oxon products were not necessarily the major transformation product. CP and its corresponding oxon were both found to be susceptible to chlorine-assisted hydrolysis (4). Since tetrahedral phosphorus atoms are known to be more susceptible to hydrolysis by supernucleophiles (33), and hypochlorite is a supernucleophile, intrinsic rate coefficients for both the chlorine-assisted hydrolysis and the HOCl-oxidation pathways need to be determined for each OP pesticide.

Degradation pathway models have been shown to be an effective tool determining rate coefficients in complex systems. Previously, researchers have used the monochloramine autodecomposition model to determine rate coefficients for the reactions of monochloramine and dichloramine with triclosan and NOM (27, 28). More applicable to this reaction system, Duirk and Collette (4) developed a degradation pathway model for CP in order to determine the intrinsic rate coefficients for both HOCl and  $\text{OCl}^-$ . Knowing that the pH dependency on the rate of OP loss is due to chlorine speciation, pooled data at pH 6.5 and 9 will be used to parameterize the intrinsic rate coefficients for HOCl ( $k_{\text{HOCl,OP}}$ ) and  $\text{OCl}^-$  ( $k_{\text{OCl,OP}}$ ) reacting with each OP pesticide using the following system of ordinary differential equations. In the following equations,  $k_{\text{OCl,OP}}$  is the intrinsic rate coefficient for hypochlorite assisting in the hydrolysis of

$$\frac{d[\text{HOCl}]_T}{dt} = -k_{\text{HOCl,OP}}[\text{HOCl}][\text{OP}] - k_{\text{OCl,OP}}[\text{OCl}^-][\text{OP}] - k_{\text{OCl,OPO}}[\text{OCl}^-][\text{OPO}] \quad (4)$$

$$\frac{d[\text{OP}]}{dt} = -k_{\text{HOCl,OP}}[\text{HOCl}][\text{OP}] - k_{\text{h,CP}}[\text{OP}] - k_{\text{OCl,OP}}[\text{OCl}^-][\text{OP}] \quad (5)$$

$$\frac{d[\text{OPO}]}{dt} = k_{\text{HOCl,OP}}[\text{HOCl}][\text{OP}] - k_{\text{h,OPO}}[\text{OPO}] - k_{\text{OCl,OPO}}[\text{OCl}^-][\text{OPO}] \quad (6)$$

$$\frac{d[\text{OPH}]}{dt} = k_{\text{h,OP}}[\text{OP}] + k_{\text{OCl,OP}}[\text{OCl}^-][\text{OP}] + k_{\text{h,OPO}}[\text{OPO}] + k_{\text{OCl,OPO}}[\text{OCl}^-][\text{OPO}] \quad (7)$$

the OPO (oxon transformation product), and  $k_{\text{h,OP}}$  and  $k_{\text{h,OPO}}$  are the rate coefficients for both OP and OPO hydrolysis, and OPH represents the hydrolysis product. Rate equations were written based on the stoichiometric equations in Table 4. For most of the OP pesticides, only equations 4 and 5 are applicable due to the inability to accurately quantify the oxon product.

The  $k_{\text{HOCl,OP}}$  were found to cluster in the range of  $1.7\text{-}2.2 \times 10^6 \text{ M}^{-1}\text{h}^{-1}$ , with CE and DZ being notable exceptions (Table 5). The  $k_{\text{OCl,OP}}$  appear to show differences between the subgroups. For the phosphorothioate subgroup,  $k_{\text{OCl,OP}}$  appears to be an order of magnitude faster than  $k_{\text{B,OP}}$  (Tables 3 and 5). However, the  $\text{OCl}^-$  does not appear to increase the rate of hydrolysis as significantly for the phosphorodithioate subgroup. This could be due to the fact that they are generally found to be extremely susceptible to nucleophilic attack from hydroxide ion. DZ is the only OP pesticide in which an intrinsic rate coefficient has been previously reported (17),  $k_{\text{HOCl,DZ}} = 4.68 \times 10^5 \text{ M}^{-1}\text{h}^{-1}$  and  $k_{\text{OCl,DZ}} = 972 \text{ M}^{-1}\text{h}^{-1}$ . Although the hypochlorite intrinsic rate coefficients were similar, HOCl rate coefficients were found to be an order of magnitude different. The difference can be explain because  $k_{\text{HOCl,DZ}}$  was approximated from data gathered only over the pH range of 9.5-11, and it was thought that both HOCl and  $\text{OCl}^-$

resulted in oxon formation. Since parallel reaction pathways can occur at any pH, the most accurate method to parameterize reaction rate coefficients of OP pesticides in the presence of chlorine would be to use a comprehensive transformation pathway model and data sets relevant to drinking water treatment conditions.

Frontier molecular orbital theory has been used to correlate oxidation rate coefficients with the easily calculated energy of highest occupied molecular orbital ( $E_{\text{HOMO}}$ ) (34).  $E_{\text{HOMO}}$  was initially thought to be able to correlate all 8 OP pesticides; however, subgroup differences were quickly unveiled (Figure 16). The phosphorodithioate subgroup was found to have a slightly higher potential than the phosphorothioate subgroup. This is most likely due to the sulfur linkage and the methyl esters at the tetrahedral phosphorus atom allowing them to be more easily oxidized by chlorine than the phosphorothioate subgroup, which primarily had ethyl and phenyl esters.  $E_{\text{HOMO}}$  was found to be a good molecular descriptor describing the oxidation of OP pesticides within each subgroup.

Other molecular descriptors were needed in order to correlate the reactivity of hypochlorite ion with each OP pesticide. Cross correlations use rate coefficients as molecular descriptors with a well understood reaction mechanism (i.e.,  $\text{S}_{\text{N}}2$  alkaline hydrolysis) and infer a mechanistically similar reaction for a different reactant (i.e., chlorine-assisted hydrolysis) (35). Therefore, correlating  $k_{\text{OCl,OP}}$  with alkaline hydrolysis rate coefficients for all 8 OP pesticides would then confirm that  $\text{OCl}^-$  acts as a nucleophile accelerating OP pesticide hydrolysis. Subgroup differences were evident as the phosphorothioates generally hydrolyze slower at alkaline pH than the phosphorodithioates (Figure 17); however, chlorine appeared to have a greater effect accelerating OP pesticide hydrolysis as indicated by the slope of the regression line being an order of magnitude greater than the slope for the phosphorodithioates. Even with the

differences between the two OP pesticide subgroups, this cross correlation validates that  $\text{OCl}^-$  acts like a nucleophile attacking the tetrahedral phosphorus atom accelerating the hydrolysis of OP pesticides. However, it is important to note that  $\text{HOCl}$  still rapidly transforms OP pesticides to their corresponding oxon at pH 9. Oxon stability in the presence of aqueous chlorine still needs to be investigated.

### 3.3 *OP Oxon Chlorine-Assisted Hydrolysis*

Chlorine assisted hydrolysis was first observed by Edwards et al., (33) investigating the factors that determine the reactivity of nucleophiles, which are basicity, polarizability, and the presence of unshared pairs of electrons on the adjacent atom to the nucleophilic atom (i.e., the alpha effect). The three lone-pairs of electrons on both the chlorine and oxygen atom enhance hypochlorite's nucleophilicity towards specific moieties such as a tetrahedral phosphorus (i.e., phosphoesters) and carbonyls. Hypochlorite is considered to be a supernucleophile towards phosphoesters because of these repulsions (36). At pH 9, DZO, MAO, and PAO loss was observed in the presence of aqueous chlorine (Figure 18). With subgroup differences aside, the loss of each oxon increased linearly proportional with increasing chlorine concentrations. DZO and PAO were significantly more stable than MAO at pH 9 because the phosphorothiolates are more susceptible to alkaline hydrolysis (8).

The rate coefficients for chlorine-assisted hydrolysis for all four oxons were found only to be slightly larger than their corresponding parents (Table 5). This was first reported with CP and CPO in the presence of chlorine and bromine (4, 20). This is due to the structure of the nucleophile,  $\text{OCl}^-$ , and not minor structural difference between a phosphorothioate and phosphate analogs (36). Since tetrahedral phosphate moieties are susceptible to  $\text{S}_{\text{N}}2$  attack by  $\text{OCl}^-$  (33), the difference in the partial positive charge at the tetrahedral phosphorus atom between (P=S) and (P=O) does not significantly influence the rate of nucleophilic attack. Therefore, chlorine-

assisted hydrolysis rates for oxons can then be assumed to be approximately the same as their corresponding parents. This could aid risk assessors estimate exposure to the more toxic oxon products as well as direct future exposure research activities related to oxon stability in drinking water distribution systems.

### **3.4 *OP Pesticide-Chlorine Model Validation***

With the available rate coefficients determined here and in cited literature, OP pesticide transformation pathways in the presence of aqueous chlorine can be predicted under drinking water conditions. Diazinon (DZ) and parathion (PA) were chosen because their corresponding oxons and hydrolysis products are commercially available. Diazinon was found to react the fastest among the OP pesticides selected (Table 5). At a pH and chlorine concentration typical of drinking water treatment, DZ was rapidly transformed to diazoxon (DZO) (Figure 19). Also, DZO is stable in the presence of chlorine for over 48 hours at neutral pH (18). At pH 8, PA was also rapidly transformed to paraoxon (PAO) (Figure 20). PAO was also found to be relatively stable at alkaline pH, as shown previously (Figure 18). This model has already been shown to adequately predict CP transformation and degradation of CPO in the presence of natural occurring aqueous constituents (i.e., bromide and natural organic matter) (20). Regulators could potentially use this model to assess potential exposure to OP pesticides and their more toxic oxon products using the structure-activity relationships in Figures 16 and 17 to estimate reaction rate coefficients across the phosphorothioate and phosphorodithioate subgroups.

### **3.5 *OP Pesticide Degradation in the Presence of Monochloramine***

Observing the direct reaction of monochloramine with analytes in solution can be very difficult at environmentally relevant concentrations. Previous work elucidating the reaction mechanism of monochloramine with bromide, cyanide, or nitrite was performed at high millimolar concentrations of the reactants (29, 37, 38). Due to the autodecomposition

mechanism of monochloramine (24), it is nearly impossible to observe the direction reaction of monochloramine with specific analytes when at environmentally relevant concentrations. Therefore, the monochloramine autodecomposition model can be used as a tool to validate proposed transformation pathways with comprehensive data sets over a range of relevant conditions.

The observed loss of each OP pesticide was assumed to be first-order with respect to each OP. Monochloramine, dichloramine, and hypochlorous acid will exist simultaneously and vary in concentration as a function of pH. Therefore, the  $k_{\text{obs}}$  presented in Figures 21 and 22 should be viewed as a function of total oxidant in the aqueous system. The observed first-order rate coefficients for CP and DZ both decreased as pH increased from 6.5 to 9 (Figure 21). This was found to be very similar to the reaction of chlorine with both CP and DZ (Figure 14). MA followed the same trend initially until approximately pH 7.5 when alkaline hydrolysis became the dominant degradation pathway (Figure 22). However, it appears that dichloramine and hypochlorous acid are primarily responsible for the loss of the OP pesticides at pH 6.5 and 7. As pH grows more alkaline, the direct reaction between monochloramine and the OP may be inconsequential compared to alkaline hydrolysis.

OP pesticide degradation pathways in the presence of monochloramine will be intimately intertwined with monochloramine autodecomposition. Since alkaline hydrolysis of MA was a significant loss pathway, further discussion on OP pesticide degradation pathways will primarily refer to CP and DZ. As pH decreased so did the observed rate of OP pesticide loss. The initial monochloramine concentration was constant for all the experiments; therefore, the direct reaction of monochloramine with OP pesticides appears to be minimal. However, near neutral pH three possible oxidants are formed due to monochloramine autodecomposition that could be

responsible for the loss of OP pesticides: hypochlorous acid (HOCl), dichloramine (NHCl<sub>2</sub>), and monochlorammonium ion (NH<sub>3</sub>Cl<sup>+</sup>). Hypochlorous acid forms primarily due to the hydrolysis of monochloramine (Table 1 reaction 2), and it does react with all three OP pesticides. However, HOCl can either react with ammonia to reform monochloramine or with monochloramine to form dichloramine (Table 1 reaction 3). Dichloramine formation is also due to monochloramine disproportionation, which is acid catalyzed Table 1 reaction 5. This acid-catalyzed reaction involves the formation of monochlorammonium ion (39).



Even though phosphate and carbonate salts participate as proton donors at high concentrations, they are several orders of magnitude less effective in the formation of monochlorammonium ion at environmentally relevant concentrations. Therefore, the primary dichloramine formation pathway will be due to HOCl reacting with NH<sub>2</sub>Cl. This can be significant because dichloramine has been found to be more reactive with cyanide, sulfite, and triclosan than monochloramine (28, 29, 38). The following are proposed additional reactions of chlorinated oxidants with OP pesticides in the presence of monochloramine.



Since hypochlorous acid is a product of monochloramine autodecomposition, all known OP degradation pathways will also be included in the partial rate expressions, equations 11-17, which are added to the full monochloramine autodecomposition model (Table 6).

$$\frac{d[\text{NH}_2\text{Cl}]}{dt} = -k_{\text{NH}_2\text{Cl},\text{OP}}[\text{NH}_2\text{Cl}][\text{OP}] + k_{\text{NHCl}_2,\text{OP}}[\text{NHCl}_2][\text{OP}] \quad (11)$$

$$\frac{d[\text{NHCl}_2]}{dt} = -k_{\text{NHCl}_2,\text{OP}}[\text{NHCl}_2][\text{OP}] \quad (12)$$



$$\frac{d[\text{HOCl}]_T}{dt} = -k_{\text{HOCl,OP}}[\text{HOCl}][\text{OP}] - k_{\text{OCl,OP}}[\text{OCl}^-][\text{OP}] - k_{\text{OCl,OPO}}[\text{OCl}^-][\text{OPO}] \quad (13)$$

$$\frac{d[\text{NH}_3]_T}{dt} = k_{\text{NHC2Cl,OP}}[\text{NH}_2\text{Cl}][\text{OP}] \quad (14)$$

$$\frac{d[\text{OP}]}{dt} = -k_{\text{HOCl,OP}}[\text{HOCl}][\text{OP}] - k_{\text{h,CP}}[\text{OP}] - k_{\text{OCl,OP}}[\text{OCl}^-][\text{OP}] \quad (15)$$

$$\frac{d[\text{OPO}]}{dt} = k_{\text{HOCl,OP}}[\text{HOCl}][\text{OP}] - k_{\text{h,OPO}}[\text{OPO}] - k_{\text{OCl,OPO}}[\text{OCl}^-][\text{OPO}] \quad (16)$$

$$\frac{d[\text{OPH}]}{dt} = k_{\text{h,OP}}[\text{OP}] + k_{\text{OCl,OP}}[\text{OCl}^-][\text{OP}] + k_{\text{h,OPO}}[\text{OPO}] + k_{\text{OCl,OPO}}[\text{OCl}^-][\text{OPO}] \quad (17)$$

Additional assumptions are that in the monochloramine-OP pesticide reaction model the reaction of monochloramine and dichloramine with each OP pesticide do not lead to oxon formation. Also, that the reactions of monochloramine and dichloramine are 1-to-1 elemental stoichiometric reactions. The reaction of dichloramine and OP pesticides results in the regeneration of monochloramine, which is similar to dichloramine reacting with inorganics (29, 38). The direct reaction of monochloramine with OP pesticides results in ammonia formation. Finally, rate coefficients determined using the monochloramine-OP pesticide reaction model exhibit no pH dependency.

Two rate coefficients need to be determined for both monochloramine and dichloramine with these OP pesticides. Since dichloramine rapidly decays above neutral pH (40), experiments to determine  $k_{\text{NH}_2\text{Cl,OP}}$  were conducted in the presence of excess ammonia at pH 8.5 to promote monochloramine stability and reformation (41). In the presence of excess ammonia ( $[\text{NH}_3]_T = 0.02\text{-}0.45$  or  $\text{Cl/N} = 0.7\text{-}0.1$  mol/mol), the rate of OP pesticide degradation decreased as ammonia concentrations increases (Figure 23). Due to MA being susceptible to alkaline

hydrolysis, MA loss at pH 8.5 was significantly faster than CP and DZ. For each pesticide, these data sets were pooled for each OP pesticide and an intrinsic rate coefficient for  $\text{NH}_2\text{Cl}$  with each OP pesticide was determined using nonlinear regression analysis. The rate coefficients found for the direct reaction of monochloramine with each OP pesticide were relatively small in magnitude (Table 7) compared to  $k_{\text{HOCl,OP}}$  (Table 5). This is not unusual because another study has reported similar results with triclosan (28). Knowing the  $k_{\text{HOCl,OP}}$  of each OP pesticide, the remaining data for each OP pesticide was pooled in order to determine  $k_{\text{NHCl}_2,\text{OP}}$ . Dichloramine was found to be two orders of magnitude great than monochloramine with each OP pesticide (Table 7), which is consistent with previously reported results (29, 38). Dichloramine appears to play a significant role in the loss of OP pesticides near neutral pH.

Using the final parameter estimates in Table 7, the monochloramine-OP pesticide reaction model was used to predict the loss of each OP pesticide in the presence of monochloramine over the pH range of 6.5-9. Hydrolysis was not a major loss pathway for either CP or DZ over this range; therefore, oxidation was the primary degradation pathway for both pesticides in the presence of monochloramine (Figures 24 and 25). The loss of CP and DZ in the presence of monochloramine was found to be relatively fast at pH 6.5 due to the formation of dichloramine and hypochlorous, which then react with the OP pesticides. As pH increased to 9, the rate of CP and DZ loss in the presence of monochloramine decreased due to: 1) the rapid disproportionation of dichloramine above neutral pH (42), 2) speciation of ammonium to ammonia which rapidly reacts with hypochlorous acid reforming monochloramine, 3) hypochlorous acid speciation to hypochlorite which does not participate in monochloramine reformation, and 4) monochloramine not being as reactive with either pesticide compared to other chlorinated oxidants. Since hydrolysis of MA is a significant degradation pathway at pH

7.5 and above, modeling MA hydrolysis was very important in order to correctly parameterize  $k_{\text{NH}_2\text{Cl,OP}}$  and  $k_{\text{NHCl}_2,\text{OP}}$ . As shown in Figure 26, the model was found very capable of predicting both monochloramine and MA concentrations. The excellent correlation between the experimental results and the model predictions indicate that the fundamental reactions responsible for the loss of both monochloramine and the OP pesticides were incorporated into the monochloramine-OP pesticide reaction model.

Unlike the chlorination experiments, only a select few OP pesticides were used in the chloramination experiments. Since CP and DZ are from the phosphorothioate subgroup and MA is from the phosphorodithioate subgroup, it is not possible to correlated the reactivity of dichloramine and monochloramine to  $E_{\text{HOMO}}$  as with  $k_{\text{HOCl,OP}}$ . However, the reactivity of the three chlorinated oxidants can be correlated to each OP pesticide using half-wave potentials ( $E_{1/2}$ ). Half-wave potentials have been shown to be a good descriptor for the electrophilicities of HOCl,  $\text{NH}_2\text{Cl}$ , and  $\text{NHCl}_2$  with organic and inorganic compounds (28); however, using half-wave potentials to correlate structure to reactivity is not as robust as thermodynamic parameters (43). Figure 27 shows a good correlation for the three oxidants with the three pesticides. It is interesting to note that the slope for each pesticide was found to be the same (slope = 0.30) with just slight differences in the intercept. This appears to indicate that degree of electrophilicity of each oxidant with each OP pesticide may be proportional across the OP pesticide class and not dependent on subgroup. Therefore, estimates for the reactivity of monochloramine and dichloramine with other OP pesticides could be made from knowing only  $k_{\text{HOCl,OP}}$  (Table 5), or the  $k_{\text{NH}_2\text{Cl,OP}}$  and  $k_{\text{NHCl}_2,\text{OP}}$  for CP or MA could be used to quickly estimate the fate of other OP pesticides in the presence on monochloramine..

Although the reaction rate coefficients of the chlorinated oxidants were found to correlate with each OP, they appear not to react via the same mechanism (i.e., reaction center). Product studies have shown that only the HOCl reaction pathway resulted in oxon formation, and that the resulting oxons also appear not to be stable in the presence of monochloramine. The reaction of monochloramine and dichloramine do not appear to result in oxon formation; however, they may react with each OP pesticide resulting in a difference transformation product while not mitigating toxicity. Additional work is needed in order to understand the fate of OP pesticides and their oxon transformation products in the presence of monochloramine.

## 4 CONCLUSION

Eight OP pesticides and three of the oxon transformation products were investigated in the presence of chlorinated oxidants. It was originally thought that by investigating a class of pesticides that structure-activity relationships could easily be developed. However, it quickly became apparent that subgroups could be correlated within each OP pesticide class; however, correlations could not be made across the chemical class. This became evident looking at hydrolysis rate coefficients for the phosphorothioate, phosphate, and the phosphorodithioate subgroups. Chlorination of all eight pesticides led to a similar conclusion. Chloramination of three of the most commonly detected OP pesticides provided some insight into how chlorinated oxidants react with OP pesticides. Overall, OP pesticide structure was found to dictate reactivity in all three systems.

Hydrolysis rate coefficients were determined for 4 pesticides due to lack of reported intrinsic rate coefficients. Pesticides from the phosphorodithioate group hydrolyzed rapidly under alkaline conditions. Also, oxons were found to be more susceptible to alkaline hydrolysis compared to the corresponding thionates due to the oxygen being more electronegative than sulfur, which facilitates the nucleophilic attack by hydroxide ion at the slightly more positively charged phosphorus atom. Also, ethyl esters appear to hinder nucleophilic attack by hydroxide ion compared to a structurally similar pesticide with methyl esters at the phosphorus atom; however, no direct comparison can be inferred for the difference in hydrolysis rates between the phosphorothioate and phosphorodithioate subgroups investigated here. Therefore, more hydrolysis studies need to be conducted at environmentally relevant conditions to determine the hydrolytic behavior of OP pesticides, which intrinsic hydrolysis rate coefficients could then be predicted via structure-activity relationships.

In the presence of aqueous chlorine, eight OP pesticides were investigated and intrinsic rate coefficients for both HOCl and OCl<sup>-</sup> were calculated. Since multiple reaction pathways occur simultaneously over the pH range of 6.5-9, a chlorine-OP pesticide reaction model previously developed for CP was used. Intrinsic rate coefficients were first found for HOCl at pH 6.5 then OCl<sup>-</sup> at pH 9. The reaction of HOCl with OP pesticides results in the rapid formation of the corresponding oxon. Hypochlorite acts as a nucleophile accelerating the hydrolysis of the OP pesticide and not resulting in oxon formation. When the intrinsic rate coefficients were correlated to molecular descriptors, subgroup differences were readily apparent. The energy of the highest occupied molecular orbital ( $E_{\text{HOMO}}$ ) showed that  $k_{\text{HOCl,OP}}$  correlated within the two subgroups. The phosphorothioates were found to be lower in energy, and the phosphorodithioates were more reactive as a group as indicated by the greater slope of the regression line. The alkaline hydrolysis rate ( $k_{\text{B,OP}}$ ) was found to correlate to  $k_{\text{OCl,OP}}$  within each OP subgroup, which also implies that the mechanism of OCl<sup>-</sup> and OH<sup>-</sup> are similar. Therefore, OCl<sup>-</sup> does attach the tetrahedral phosphorus as a nucleophile accelerating the hydrolysis of all eight OP pesticides and three oxons.

Three of the most commonly detected OP pesticides (CP, DZ, and MA) in drinking water supplies were examined in presence of chloramines. The loss of all three pesticides under chloramination conditions was found to be highly pH dependent. At pH 6.5, the primary degradation pathway for OP pesticides was due to reaction with dichloramine and hypochlorous acid, which are formed during monochloramine autodecomposition. The direct reaction of monochloramine with each OP pesticide was found to be a minimal degradation pathway, which was confirmed when parameterizing  $k_{\text{NH}_2\text{Cl,OP}}$  for each OP pesticide in the presence of excess ammonia. The order of reactivity for the three chlorinated oxidants with each OP pesticide was

$\text{HOCl} \gg \text{NHCl}_2 \gg \text{NH}_2\text{Cl}$ . The reactivity of the three chlorinated oxidants correlated with half-wave potentials ( $E_{1/2}$ ) for each OP pesticide.

The stability of OP pesticides was investigated under conditions similar to drinking water treatment. The eight pesticides in this study showed that reaction parameters could not be correlated across the OP pesticide class, but correlations could be made within subgroups indicating that minute structure differences can significantly impact reactivity. Structure-activity relationships developed here can allow for the prediction of critical reaction parameters of OP pesticides in the presence of chlorinated oxidants. Along with the presented model, regulators could access the potential risk associated when consuming potable water contaminated with OP pesticides.

## 5 REFERENCES

1. Kolpin, D. W.; Barbash, J. E.; Gilliom, R. J., Pesticides in ground water of the United States, 1992-1996. *Ground Water* **2000**, 38, (6), 858-863.
2. Verstraeten, I. M.; Thurman, E. M.; Lindsey, M. E.; Lee, E. C.; Smith, R. D., Changes in concentrations of triazine and acetamide herbicides by bank filtration, ozonation, and chlorination in a public water supply. *Journal of Hydrology* **2003**, 276, (1-4), 287-288.
3. Coupe, R. H.; Blomquist, J. D., Water-soluble pesticides in finished water of community water supplies. *Journal American Water Works Association* **2004**, 96, (10), 56-68.
4. Duirk, S. E.; Collette, T. W., Degradation of Chlorpyrifos in Aqueous Chlorine Solutions: Pathways, Kinetics, and Modeling. *Environmental Science and Technology* **2006**, 40, 546-551.
5. Pehkonen, S. O.; Zhang, Q., The degradation of organophosphorus pesticides in natural waters: A critical review. *Critical Reviews in Environmental Science and Technology* **2002**, 32, (1), 17-72.
6. Wolfe, N. L.; Zepp, R. G.; Baughman, G. L.; Gordon, J. A., Kinetic Investigation of Malathion Degradation in Water. *Bulletin of Environmental Contamination and Toxicology* **1975**, 13, (6), 707-713.
7. Wolfe, N. L.; Zepp, R. G.; Gordon, J. A.; Baughman, G. L.; Cline, D. M., Kinetic of Chemical Degradation of Malathion in Water. *Environ. Sci. Technol.* **1977**, 11, (1), 88-93.
8. Faust, S. D.; Gomaa, H. M., Chemical Hydrolysis of Some Organic Phosphorus and Carbamate Pesticides in Aquatic Environments. *Environmental Letters* **1972**, 3, (3), 171-201.
9. Macalady, D. L.; Wolfe, N. L., New Perspectives on the Hydrolytic Degradation of the Organophosphorothioate Insecticide Chlorpyrifos. *Journal of Agricultural and Food Chemistry* **1983**, 31, (6), 1139-1147.
10. *Community Water System Survey*. United States Environmental Protection Agency: 1997; Vol. 1, EPA 815-R-97-011a.
11. Lopez, A.; Mascolo, G.; Tiravanti, G.; Santori, M.; Passino, R., Oxidation of Sulfur-Containing S-Triazines During Groundwater Hypochlorination. *Water Science and Technology* **1994**, 30, (7), 53-59.
12. Mascolo, G.; Lopez, A.; Passino, R.; Ricco, G.; Tiravanti, G., Degradation of Sulfur-Containing S-Triazines During Water Chlorination. *Water Res.* **1994**, 28, (12), 2499-2506.



13. Adams, C. D.; Randtke, S. J., Removal of Atrazine from Drinking-Water by Ozonation. *Journal American Water Works Association* **1992**, 84, (9), 91-102.
14. Miles, C. J., Degradation of Aldicarb, Aldicarb Sulfoxide, and Aldicarb Sulfone in Chlorinated Water. *Environ. Sci. Technol.* **1991**, 25, (10), 1774-1779.
15. Mason, Y. Z.; Choshen, E.; Ravacha, C., Carbamate Insecticides - Removal from Water by Chlorination and Ozonation. *Water Res.* **1990**, 24, (1), 11-21.
16. Kodama, S.; Yamamoto, A.; Matsunaga, A., S-Oxygenation of thiobencarb in tap water processed by chlorination. *Journal of Agricultural and Food Chemistry* **1997**, 45, (3), 990-994.
17. Zhang, Q.; Pehkonen, S. O., Oxidation of diazinon by aqueous chlorine: Kinetics, mechanisms, and product studies. *Journal of Agricultural and Food Chemistry* **1999**, 47, (4), 1760-1766.
18. Magara, Y.; Aizawa, T.; Matumoto, N.; Souna, F., Degradation of Pesticides by Chlorination During Water-Purification. *Water Science and Technology* **1994**, 30, (7), 119-128.
19. Wu, J. G.; Laird, D. A., Abiotic transformation of chlorpyrifos to chlorpyrifos oxon in chlorinated water. *Environmental Toxicology and Chemistry* **2003**, 22, (2), 261-264.
20. Duirk, S. E.; Tarr, J. C.; Collette, T. W., Chlorpyrifos transformation by aqueous chlorine in the presence of bromide and natural organic matter. *Journal of Agricultural and Food Chemistry* **2008**, 56, (4), 1328-1335.
21. Pinkston, K. E.; Sedlak, D. L., Transformation of aromatic ether-and amine-containing pharmaceuticals during chlorine disinfection. *Environ. Sci. Technol.* **2004**, 38, (14), 4019-4025.
22. Chen, W. H.; Young, T. M., NDMA formation during chlorination and chloramination of aqueous diuron solutions. *Environ. Sci. Technol.* **2008**, 42, (4), 1072-1077.
23. Chen, Z.; Valentine, R. L., Modeling the formation of N-nitrosodimethylamine (NDMA) from the reaction of natural organic matter (NOM) with monochloramine. *Environ. Sci. Technol.* **2006**, 40, (23), 7290-7297.
24. Jafvert, C. T.; Valentine, R. L., Reaction Scheme for the Chlorination of Ammoniacal Water. *Environ. Sci. Technol.* **1992**, 26, (3), 577-586.
25. Duirk, S. E.; Gombert, B.; Croue, J. P.; Valentine, R. L., Modeling monochloramine loss in the presence of natural organic matter. *Water Res.* **2005**, 39, (14), 3418-3431.

26. Duirk, S. E.; Valentine, R. L., Modeling dichloroacetic acid formation from the reaction of monochloramine with natural organic matter. *Water Res.* **2006**, *40*, (14), 2667-2674.
27. Duirk, S. E.; Valentine, R. L., Bromide oxidation and formation of dihaloacetic acids in chloraminated water. *Environ. Sci. Technol.* **2007**, *41*, (20), 7047-7053.
28. Greychock, A. E.; Vikesland, P. J., Triclosan reactivity chloraminated waters. *Environ. Sci. Technol.* **2006**, *40*, (8), 2615-2622.
29. Schurter, L. M.; Bachelor, P. P.; Margerum, D. W., Nonmetal Redox Kinetics: Mono-, Di-, and Trichloramine Reactions with Cyanide Ion. *Environ. Sci. Technol.* **1995**, *29*, (4), 1127-1134.
30. *Standard Methods for the Examination of Water and Wastewater*. 20th ed.; APHA, AWWA and WEF: Washington D. C., 1998.
31. Wolfe, N. L., Organo-Phosphate and Organophosphorothionate Esters - Application of Linear Free-Energy Relationships to Estimate Hydrolysis Rate Constants for Use in Environmental Fate Assessment. *Chemosphere* **1980**, *9*, (9), 571-579.
32. Snoeyink, V. L.; Jenkins, D. A., *Water Chemistry*. John Wiley & Sons: New York, NY, 1980.
33. Edwards, J. O.; Pearson, R. G., Factors Determining Nucleophilic Reactivities. *Journal of the American Chemical Society* **1962**, *84*, (1), 16-24.
34. Hu, J. Y.; Morita, T.; Magara, Y.; Aizawa, T., Evaluation of reactivity of pesticides with ozone in water using the energies of frontier molecular orbitals. *Water Res.* **2000**, *34*, (8), 2215-2222.
35. Canonica, S.; Tratnyek, P. G., Quantitative structure-activity relationships for oxidation reactions of organic chemicals in water. *Environmental Toxicology and Chemistry* **2003**, *22*, (8), 1743-1754.
36. England, W. B.; Kovacic, P.; Hanrahan, S. M.; Jones, M. B., Molecular-Orbital Theory of Supernucleophiles - Complementary Criteria and Supporting Evidence. *Journal of Organic Chemistry* **1980**, *45*, (11), 2057-2063.
37. Margerum, D. W.; Schurter, L. M.; Hobson, J.; Moore, E. E., Water Chlorination Chemistry - Nonmetal Redox Kinetics of Chloramine and Nitrite Ion. *Environ. Sci. Technol.* **1994**, *28*, (2), 331-337.
38. Yiin, B. S.; Walker, D. M.; Margerum, D. W., Nonmetal Redox Kinetics: General Acid Assisted Reactions of Chloramine with Sulfite and Hydrogen Sulfite. *Inorganic Chemistry* **1987**, *26*, (21), 3435-3441.

39. Gray, E. T.; Margerum, D. W.; Huffman, R. P., Chloramine Equilibria and the Kinetics of Disproportionation in Aqueous Solution. In *Organometals and Organometalloids: Occurance and Fate in the Environment*, Brinkman, F. E.; Bellama, J. M., Eds. ACS Books: Washington D.C., 1978; pp 264-277.
40. Vikesland, P. J.; Ozekin, K.; Valentine, R. L., Monochloramine decay in model and distribution system waters. *Water Res.* **2001**, 35, (7), 1766-1776.
41. Qiang, Z. M.; Adams, C. D., Determination of monochloramine formation rate constants with stopped-flow spectrophotometry. *Environ. Sci. Technol.* **2004**, 38, (5), 1435-1444.
42. Jafvert, C. T.; Valentine, R. L., Dichloramine Decomposition in the Presence of Excess Ammonia. *Water Res.* **1987**, 21, (8), 967-973.
43. Tratnyek, P. G.; Hoigne, J., Kinetics of Reaction of Chlorine Dioxide (OClO) in Water: 2. Quantitative Structure-Activity Relationships for Phenolic Compounds. *Water Res.* **1994**, 28, (1), 57-66.
44. Morris, J. C.; Isaac, R. A., A Critical Review of Kinetic and Thermodynamic Constants for the Aqueous Chlorine-Ammonia System. In *Water Chlorination Chemistry: Environmental Impact and Health Effects*, Jolley, R. L.; Burns, W. A.; Coutrovo, J. A.; Cumming, R. B.; Mattice, J. S.; Jacobs, V. A., Eds. Ann Arbor Science: Ann Arbor, MI, 1981; Vol. 4, pp 49-62.
45. Margerum, D. W.; Gray, E. T.; Huffman, R. P., Chlorination and the Formation of N-Chloro Compounds in Water Treatment. In *Organometals and Organometalloids: Occurance and Fate in the Environment*, Brinkman, F. E.; Bellama, J. M., Eds. ACS Books: Washington D.C., 1978; pp 278-290.
46. Hand, V. C.; Margerum, D. W., Kinetics and Mechanisms of the Decomposition of Dichloramine in Aqueous-Solution. *Inorganic Chemistry* **1983**, 22, (10), 1449-1456.
47. Leao, S. F. Kinetics of Combined Chlorine: Reactions of Substitution and Redox. University of California Berkeley, Berkeley, CA, 1981.
48. *CRC Handbook of Pesticides*. CRC Press: Boca Raton, FL, 1995.
49. Piela, B.; Wrona, P. K., Electrochemical behavior of chloramines on the rotating platinum and gold electrodes. *Journal of the Electrochemical Society* **2003**, 150, (5), E255-E265.

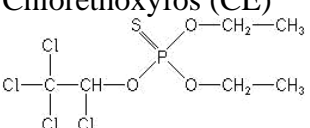
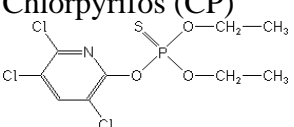
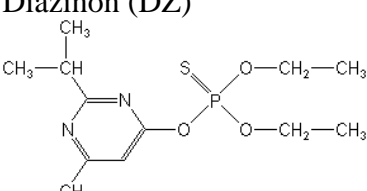
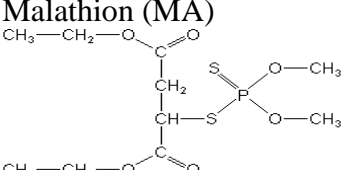
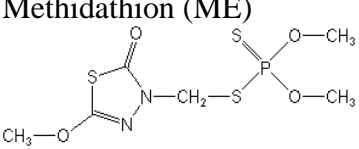
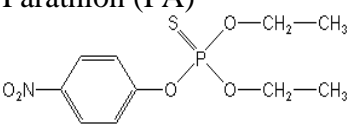
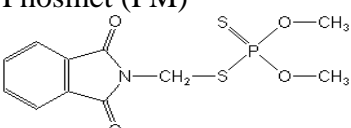
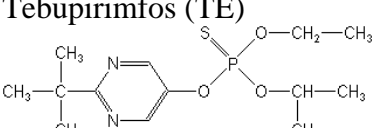
## **TABLES**

Table 1 Stoichiometric equations and coefficients in the monochloramine autodecomposition model.

Reaction	Stoichiometry	Rate/Equilibrium Coefficients (25 °C)	Reference
1	$\text{HOCl} + \text{NH}_3 \longrightarrow \text{NH}_2\text{Cl} + \text{H}_2\text{O}$	$k_1 = 1.5 \times 10^{10} \text{ M}^{-1} \text{ h}^{-1}$	(44)
2	$\text{NH}_2\text{Cl} + \text{H}_2\text{O} \longrightarrow \text{HOCl} + \text{NH}_3$	$k_2 = 7.6 \times 10^{-2} \text{ h}^{-1}$	(44)
3	$\text{HOCl} + \text{NH}_2\text{Cl} \longrightarrow \text{NHCl}_2 + \text{H}_2\text{O}$	$k_3 = 1.0 \times 10^6 \text{ M}^{-1} \text{ h}^{-1}$	(45)
4	$\text{NHCl}_2 + \text{H}_2\text{O} \longrightarrow \text{HOCl} + \text{NH}_2\text{Cl}$	$k_4 = 2.3 \times 10^{-3} \text{ h}^{-1}$	(45)
5	$\text{NH}_2\text{Cl} + \text{NH}_2\text{Cl} \longrightarrow \text{NHCl}_2 + \text{NH}_3$	$^a k_5 = \text{pH dependent}$	(40)
6	$\text{NHCl}_2 + \text{NH}_3 \longrightarrow \text{NH}_2\text{Cl} + \text{NH}_2\text{Cl}$	$k_6 = 2.16 \times 10^8 \text{ M}^{-2} \text{ h}^{-1}$	(46)
7	$\text{NH}_2\text{Cl} + \text{NHCl}_2 \longrightarrow \text{N}_2 + 3\text{H}^+ + 3\text{Cl}^-$	$k_7 = 55.0 \text{ M}^{-1} \text{ h}^{-1}$	(47)
8	$\text{NHCl}_2 + \text{H}_2\text{O} \longrightarrow ^b\text{I} + 2\text{HCl}$	$k_8 = 4.0 \times 10^5 \text{ M}^{-1} \text{ h}^{-1}$	(42)
9	$^b\text{I} + \text{NHCl}_2 \longrightarrow \text{HOCl} + \text{N}_2 + \text{HCl}$	$k_9 = 1.0 \times 10^8 \text{ M}^{-1} \text{ h}^{-1}$	(47)
10	$^b\text{I} + \text{NH}_2\text{Cl} \longrightarrow \text{N}_2 + \text{H}_2\text{O} + \text{HCl}$	$k_{10} = 3.0 \times 10^7 \text{ M}^{-1} \text{ h}^{-1}$	(47)
11	$\text{HOCl} \rightleftharpoons \text{H}^+ + \text{OCl}^-$	$\text{pK}_a = 7.5$	(32)
12	$\text{NH}_4^+ \rightleftharpoons \text{H}^+ + \text{NH}_3$	$\text{pK}_a = 9.3$	(32)
13	$\text{H}_2\text{CO}_3 \rightleftharpoons \text{H}^+ + \text{HCO}_3^-$	$\text{pK}_a = 6.3$	(32)
14	$\text{HCO}_3^- \rightleftharpoons \text{H}^+ + \text{CO}_3^{2-}$	$\text{pK}_a = 10.3$	(32)

Note:  $^a k_5 = k_{\text{H}^+} [\text{H}^+] + k_{\text{H}_2\text{CO}_3} [\text{H}_2\text{CO}_3] + k_{\text{HCO}_3^-} [\text{HCO}_3^-]$ :  $k_{\text{H}^+} = 2.5 \times 10^7 \text{ M}^{-2} \text{ h}^{-1}$ ,  $k_{\text{H}_2\text{CO}_3} = 4.0 \times 10^3 \text{ M}^{-2} \text{ h}^{-1}$ , and  $k_{\text{HCO}_3^-} = 800 \text{ M}^{-2} \text{ h}^{-1}$  at 25 °C.  $^b\text{I}$ : reactive intermediate.

Table 2 Structures and some chemical properties of select OP Pesticides (48).

Structure and Name	Log K <sub>ow</sub>	Vapor Pressure (mm Hg)	Water Solubility At 20°C (mg/L)
<b>Chlorethoxyfos (CE)</b> 	4.59	$8.25 \times 10^{-4}$	$2.0 \times 10^0$
<b>Chlorpyrifos (CP)</b> 	5.11	$1.85 \times 10^{-5}$	$2.0 \times 10^0$
<b>Diazinon (DZ)</b> 	3.81	$1.2 \times 10^{-2}$	$4.0 \times 10^1$
<b>Malathion (MA)</b> 	2.36	$7.9 \times 10^{-6}$	$1.4 \times 10^2$
<b>Methidathion (ME)</b> 	2.5	$1.88 \times 10^{-6}$	$2.0 \times 10^2$
<b>Parathion (PA)</b> 	3.83	$9.7 \times 10^{-6}$	$6.5 \times 10^0$
<b>Phosmet (PM)</b> 	2.95	$6.4 \times 10^{-1}$	$2.5 \times 10^1$
<b>Tebupirimfos (TE)</b> 	<sup>a</sup> NA	$3.75 \times 10^{-5}$	$5.5 \times 10^0$

<sup>a</sup>NA means not available.

Table 3 Neutral and alkaline hydrolysis rate coefficients for 8 OP pesticides and 3 oxon transformation products. 95% confidence intervals shown in parentheses.

OP Pesticide	$k_{N,OP}$ at 25 °C (h <sup>-1</sup> )	$k_{B,OP}$ at 25 °C (M <sup>-1</sup> h <sup>-1</sup> )	References
Chlorethoxyfos (CE)	4.68(±0.69) × 10 <sup>-4</sup>	1.25(±0.30) × 10 <sup>3</sup>	this work
Chlorpyrifos (CP)	3.72 × 10 <sup>-4</sup>	37.1	(9)
Chlorpyrifos oxon (CPO)	2.13 × 10 <sup>-3</sup>	230.2	(4)
Diazinon (DZ)	1.56 × 10 <sup>-4</sup>	18.9	(8)
Diazoxon (DZO)	9.99 × 10 <sup>-4</sup>	165.6	
Malathion (MA)	<sup>a</sup> 7.92 × 10 <sup>-5</sup>	1.98 × 10 <sup>3</sup>	(6)
Methidathion (ME)	<sup>a</sup> 1.42(±1.01) × 10 <sup>-3</sup>	2.22(±0.04) × 10 <sup>2</sup>	this work
Parathion (PA)	2.66 × 10 <sup>-4</sup>	4.3	(8)
Paraoxon (PAO)	2.00 × 10 <sup>-4</sup>	46.1	
Phosmet (PM)	<sup>b</sup> 5.55(±0.11) × 10 <sup>-4</sup>	2.73(±0.08) × 10 <sup>5</sup>	this work
Tebupirimfos (TE)	1.10(±0.01) × 10 <sup>-3</sup>	6.0(±0.1)	this work

<sup>a</sup>MA hydrolysis rate coefficient at pH 4

<sup>b</sup>PM hydrolysis rate coefficient at pH 2

Table 4 Stoichiometric equations used in the chlorine-OP pesticide transformation pathway model.

	Reaction Stoichiometry	Rate/Equilibrium Coefficient (25 °C)	Reference
1	$5\text{HOCl} + \text{OP} \xrightarrow{k_{\text{HOCl,OP}}} \text{OPO} + 5\text{H}^+ + 5\text{Cl}^- + \text{SO}_4^{2-}$	$k_{\text{HOCl,OP}} = \text{Table 5}$	this work
2	$\text{OP} \xrightarrow{k_{\text{h,OP}}} \text{OPH}$	$k_{\text{h,OP}} = k_{\text{N,OP}} + k_{\text{B,OP}}[\text{OH}^-]$ $k_{\text{N,OP}} = \text{Table 3}$ $k_{\text{B,OP}} = \text{Table 3}$	
3	$\text{OPO} \xrightarrow{k_{\text{h,OPO}}} \text{OPH}$	$k_{\text{h,OPO}} = k_{\text{N,OPO}} + k_{\text{B,OPO}}[\text{OH}^-]$ $k_{\text{N,OPO}} = \text{Table 3}$ $k_{\text{B,OPO}} = \text{Table 3}$	
4	$\text{OP} + \text{OCl}^- \xrightarrow{k_{\text{OCl,OP}}} \text{OPH}$	$k_{\text{OCl,OP}} = \text{Table 5}$	this work
5	$\text{OPO} + \text{OCl}^- \xrightarrow{k_{\text{OCl,OPO}}} \text{OPH}$	$k_{\text{OCl,OPO}} = \text{Table 5}$	this work
6	$\text{HOCl} \rightleftharpoons \text{H}^+ + \text{OCl}^-$	$\text{pK}_a = 7.5 (\text{HOCl}/\text{OCl}^-)$	(32)



Table 5      Oxidation and chlorine-assisted hydrolysis rate coefficients for 8 OP pesticides and 3 oxon transformation products. 95% confidence intervals shown in parentheses.

OP pesticide	$k_{\text{HOCl,OP}}$ at 25 °C ( $\text{M}^{-1}\text{h}^{-1}$ )	$k_{\text{OCl,OP}}$ or $k_{\text{OCl,OPO}}$ at 25 °C ( $\text{M}^{-1}\text{h}^{-1}$ )	References
Chlorethoxyfos (CE)	$0.86(\pm 0.18) \times 10^6$	$15,900 \pm 2100$	this work
Chlorpyrifos (CP) Chlorpyrifos oxon (CPO)	$1.72 \times 10^6$	990 1340	(4)
Diazinon (DZ) Diazoxon (DZO)	$3.56(\pm 0.65) \times 10^6$	$627 \pm 30$ $914.1 \pm 54.2$	this work
Malathion (MA) Malaoxon (MAO)	$1.72(\pm 0.36) \times 10^6$	$382 \pm 26$ $565 \pm 99$	this work
Methidathion (ME)	$1.89(\pm 0.12) \times 10^6$	$252 \pm 47$	this work
Parathion (PA) Paraoxon (PAO)	$2.20(\pm 0.53) \times 10^6$	$37 \pm 10$ $48 \pm 10$	this work
Phosmet (PM)	$2.84(\pm 0.80) \times 10^6$	$1000 \pm 100$	this work
Tebupirimfos (TE)	$1.76(\pm 0.43) \times 10^6$	$71 \pm 13$	this work

Table 6 Differential equations for the monochloramine autodecomposition model.

---

1)	$\frac{d[\text{NH}_2\text{Cl}]}{dt} = k_1[\text{NH}_3][\text{HOCl}] - k_2[\text{NH}_2\text{Cl}] - k_3[\text{HOCl}][\text{NH}_2\text{Cl}] + k_4[\text{NHCl}_2] -$ $2k_5[\text{NH}_2\text{Cl}]^2 + k_6[\text{NHCl}_2][\text{NH}_3] - k_7[\text{NHCl}_2][\text{NH}_2\text{Cl}] - k_{10}[\text{I}][\text{NH}_2\text{Cl}]$
2)	$\frac{d[\text{NHCl}_2]}{dt} = k_3[\text{HOCl}][\text{NH}_2\text{Cl}] - k_4[\text{NHCl}_2] + k_5[\text{NH}_2\text{Cl}]^2 - k_6[\text{H}^+][\text{NH}_3][\text{NHCl}_2]$ $k_7[\text{NH}_2\text{Cl}][\text{NHCl}_2] - k_8[\text{NHCl}_2][\text{OH}^-] - k_9[\text{I}][\text{NHCl}_2]$
3)	$\frac{d[\text{TOTOCl}]}{dt} = -k_1[\text{HOCl}][\text{NH}_3] + k_2[\text{NH}_2\text{Cl}] - k_3[\text{HOCl}][\text{NH}_2\text{Cl}] + k_4[\text{NHCl}_2] +$ $k_9[\text{I}][\text{NHCl}_2]$
4)	$\frac{d[\text{TOTNH}_3]}{dt} = -k_1[\text{HOCl}][\text{NH}_3] + k_2[\text{NH}_2\text{Cl}] + k_5[\text{NH}_2\text{Cl}]^2 - k_6[\text{NHCl}_2][\text{NH}_3]$
5)	$\frac{d[\text{Cl}^-]}{dt} = 3k_7[\text{NH}_2\text{Cl}]^2 + 2k_8[\text{NHCl}_2] + k_9[\text{I}][\text{NHCl}_2] + k_{10}[\text{I}][\text{NH}_2\text{Cl}]$
6)	$\frac{d[\text{I}]}{dt} = k_8[\text{NHCl}_2][\text{OH}^-] - k_9[\text{I}][\text{NHCl}_2] + k_{10}[\text{I}][\text{NH}_2\text{Cl}]$
7)	$\frac{d[\text{N}_2]}{dt} = k_7[\text{NH}_2\text{Cl}][\text{NHCl}_2] + k_9[\text{I}][\text{NHCl}_2] + k_{10}[\text{I}][\text{NH}_2\text{Cl}]$
8)	$\frac{d[\text{pH}]}{dt} = -(3k_7[\text{NH}_2\text{Cl}][\text{NHCl}_2] + 3k_9[\text{I}][\text{NHCl}_2] + 3k_{10}[\text{I}][\text{NH}_2\text{Cl}] +$ $k_1[\text{NH}_3][\text{HOCl}](\alpha_o\text{NH}_4 - \alpha_1\text{OCl}^-) + k_2(\alpha_1\text{OCl} - \alpha_o\text{NH}_4)[\text{NH}_2\text{Cl}] +$ $k_3[\text{NH}_2\text{Cl}][\text{HOCl}](-\alpha_1\text{OCl}^-) + k_4[\text{NHCl}_2](\alpha_1\text{OCl}^-) +$ $k_5[\text{NH}_2\text{Cl}]^2(-\alpha_o\text{NH}_4) + k_6[\text{H}^+][\text{NH}_3][\text{NHCl}_2](\alpha_o\text{NH}_4)) / \beta$

---

Table 7      Intrinsic rate coefficients for monochloramine and dichloramine reacting with CP, DZ, and MA. 95% confidence intervals shown in parentheses.

OP Pesticide	$k_{\text{NH}_2\text{Cl,OP}}$ ( $\text{M}^{-1}\text{h}^{-1}$ )	$k_{\text{NHCl}_2,\text{OP}}$ ( $\text{M}^{-1}\text{h}^{-1}$ )
Chlorpyrifos (CP)	11.2( $\pm 1.2$ )	2700( $\pm 100$ )
Diazinon (DZ)	21.4( $\pm 1.9$ )	2930( $\pm 120$ )
Malathion (MA)	10.6( $\pm 0.6$ )	2000( $\pm 200$ )

## **FIGURES**

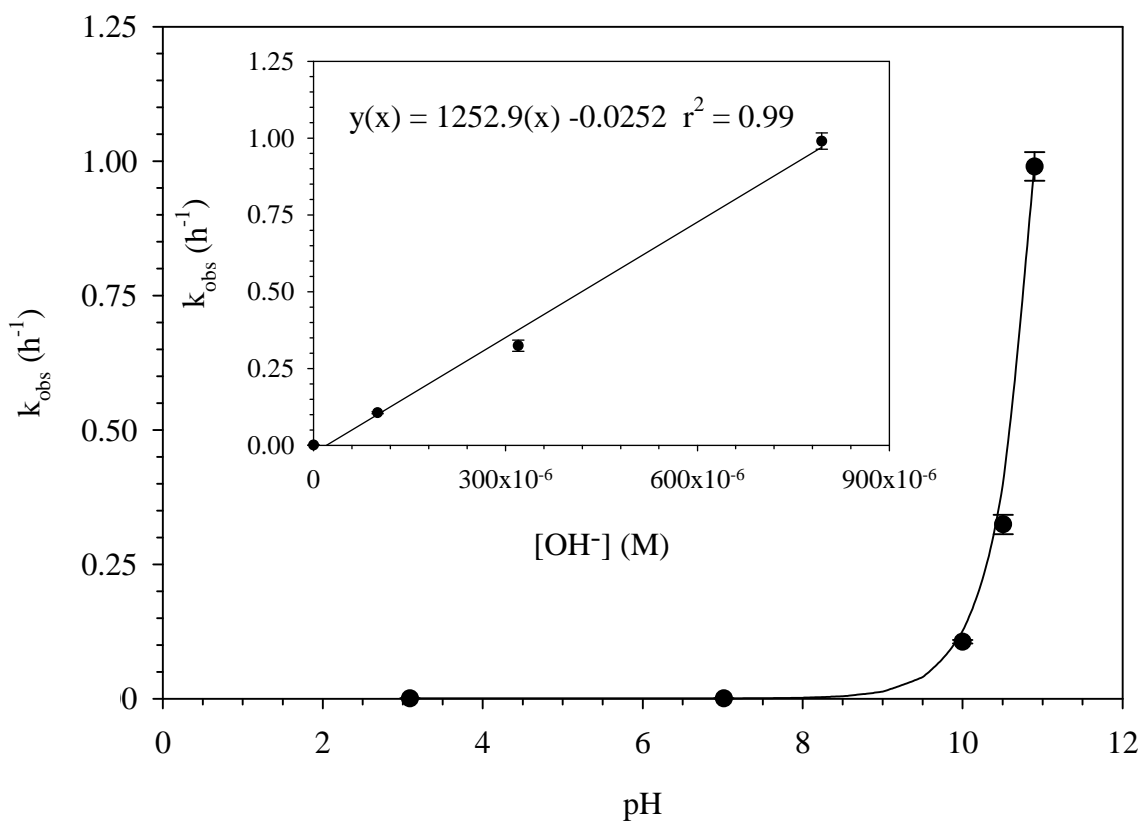


Figure 1 Hydrolytic behavior of chlorethoxyfos (CE) over the pH range of 3-11. Insert: slope represents the alkaline hydrolysis rate coefficient.  $[\text{CE}]_0 = 0.5 \mu\text{M}$ ,  $[\text{Buffer}]_T = 10 \text{ mM}$ , and Temperature =  $25 \pm 1^\circ\text{C}$ . Error bars represent 95% confidence intervals.

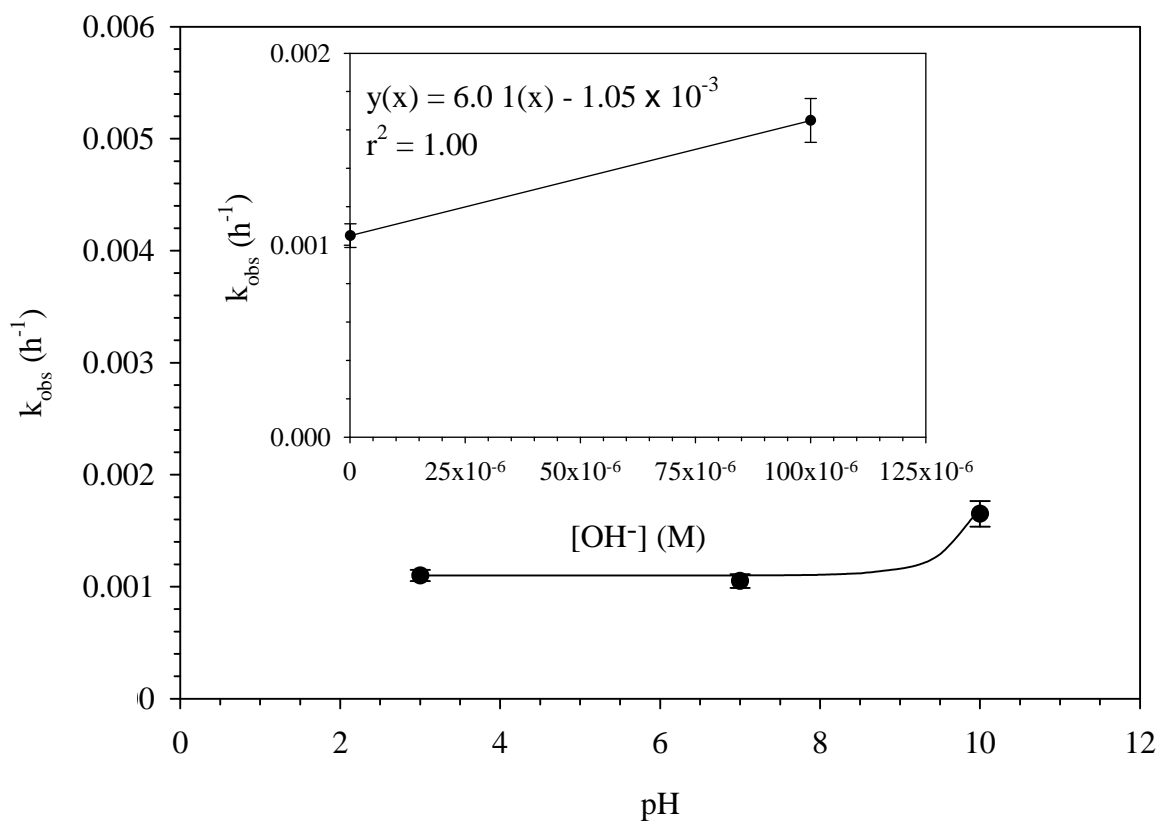


Figure 2 Hydrolytic behavior of tebupirimfos (TE) over the pH range of 3-10. Insert: slope represents the alkaline hydrolysis rate coefficient.  $[\text{TE}]_0 = 0.5 \mu\text{M}$ ,  $[\text{Buffer}]_T = 10 \text{ mM}$ , and Temperature =  $25 \pm 1^\circ\text{C}$ . Error bars represent 95% confidence intervals.

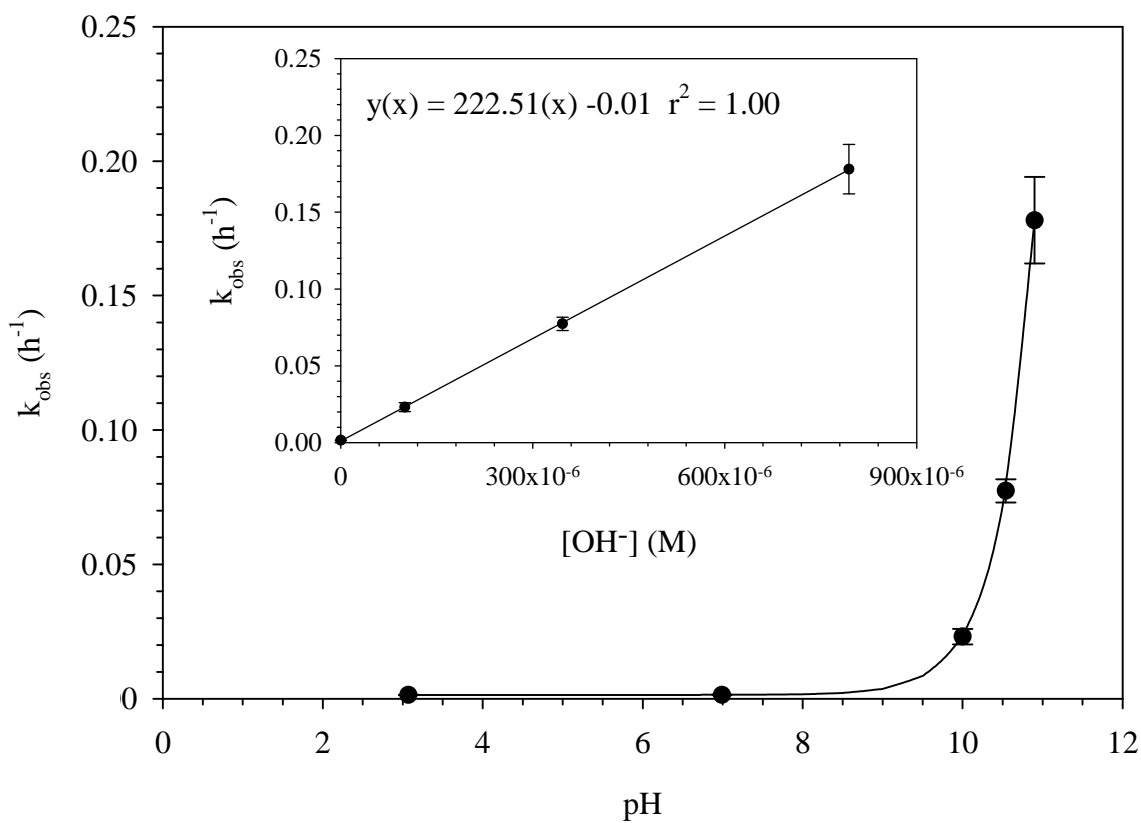


Figure 3 Hydrolytic behavior of methidathion (ME) over the pH range of 3-11. Insert: slope represents the alkaline hydrolysis rate coefficient.  $[\text{ME}]_0 = 0.5 \mu\text{M}$ ,  $[\text{Buffer}]_T = 10 \text{ mM}$ , and Temperature =  $25 \pm 1^\circ\text{C}$ . Error bars represent 95% confidence intervals.

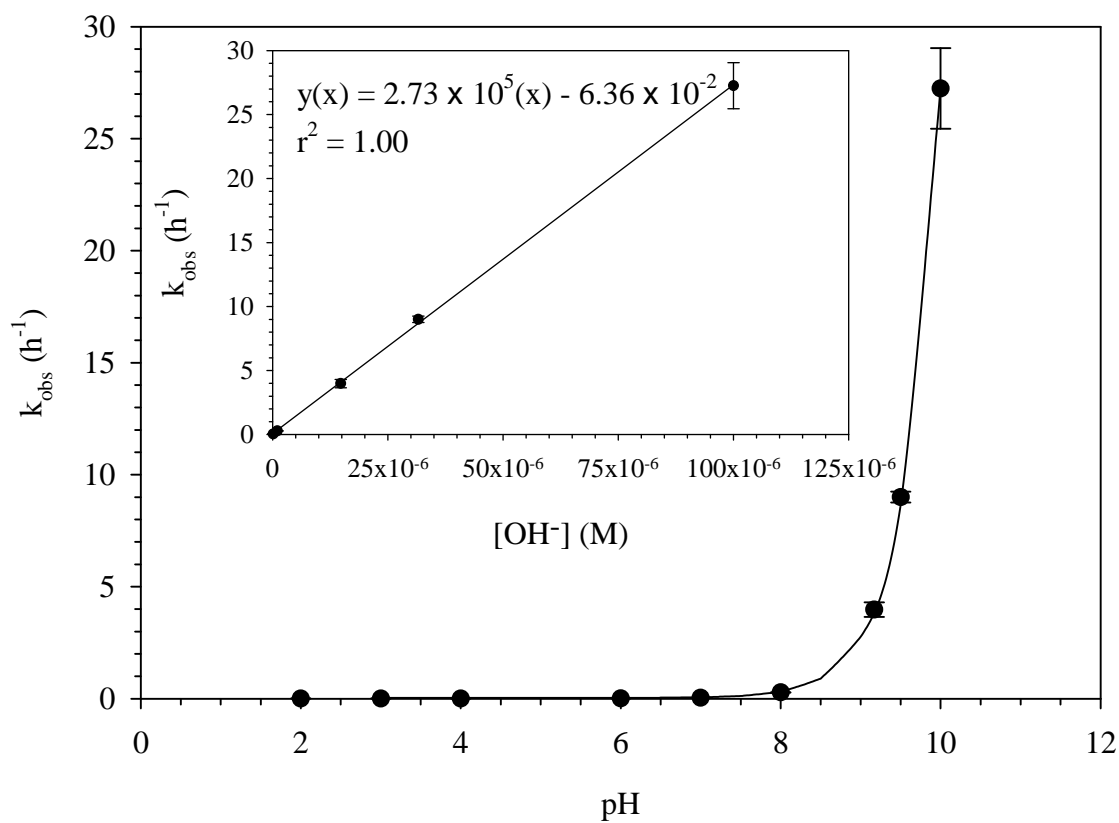


Figure 4 Hydrolytic behavior of phosmet (PM) over the pH range of 2-10. Insert: slope represents the alkaline hydrolysis rate coefficient.  $[\text{PM}]_0 = 0.5 \mu\text{M}$ ,  $[\text{Buffer}]_T = 10 \text{ mM}$ , and Temperature =  $25 \pm 1^\circ\text{C}$ . Error bars represent 95% confidence intervals.



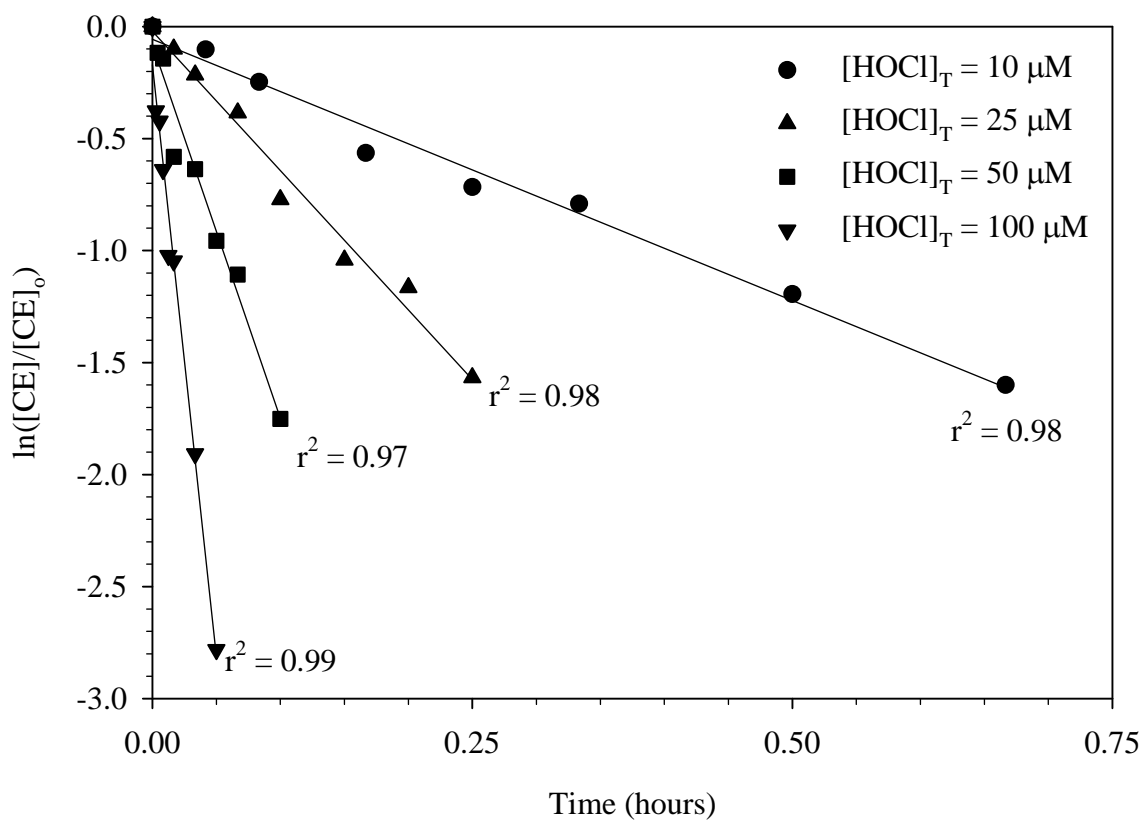


Figure 5 Observed first-order rate of CE loss in the presence of aqueous chlorine at pH 6.5.  $[\text{CE}]_0 = 0.5 \mu\text{M}$ ,  $[\text{HOCl}]_0 = 10\text{-}100 \mu\text{M}$ ,  $[\text{PO}_4]_{\text{T}} = 10 \text{ mM}$ , and Temperature =  $25 \pm 1^\circ\text{C}$ . Experiments performed in triplicate.

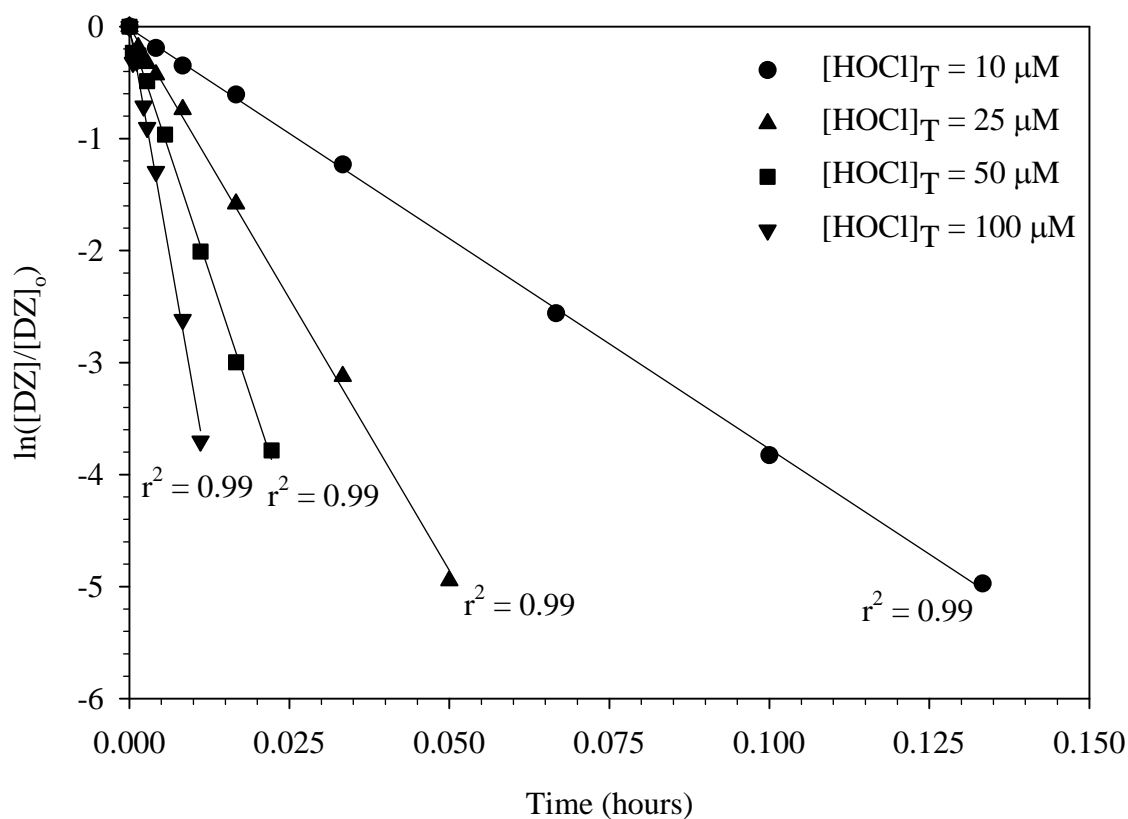


Figure 6 Observed first-order rate of DZ loss in the presence of aqueous chlorine at pH 6.5.  $[DZ]_0 = 0.5 \mu M$ ,  $[HOCl]_0 = 10\text{--}100 \mu M$ ,  $[PO_4]_T = 10 \text{ mM}$ , and Temperature =  $25 \pm 1^\circ C$ . Experiments performed in triplicate.

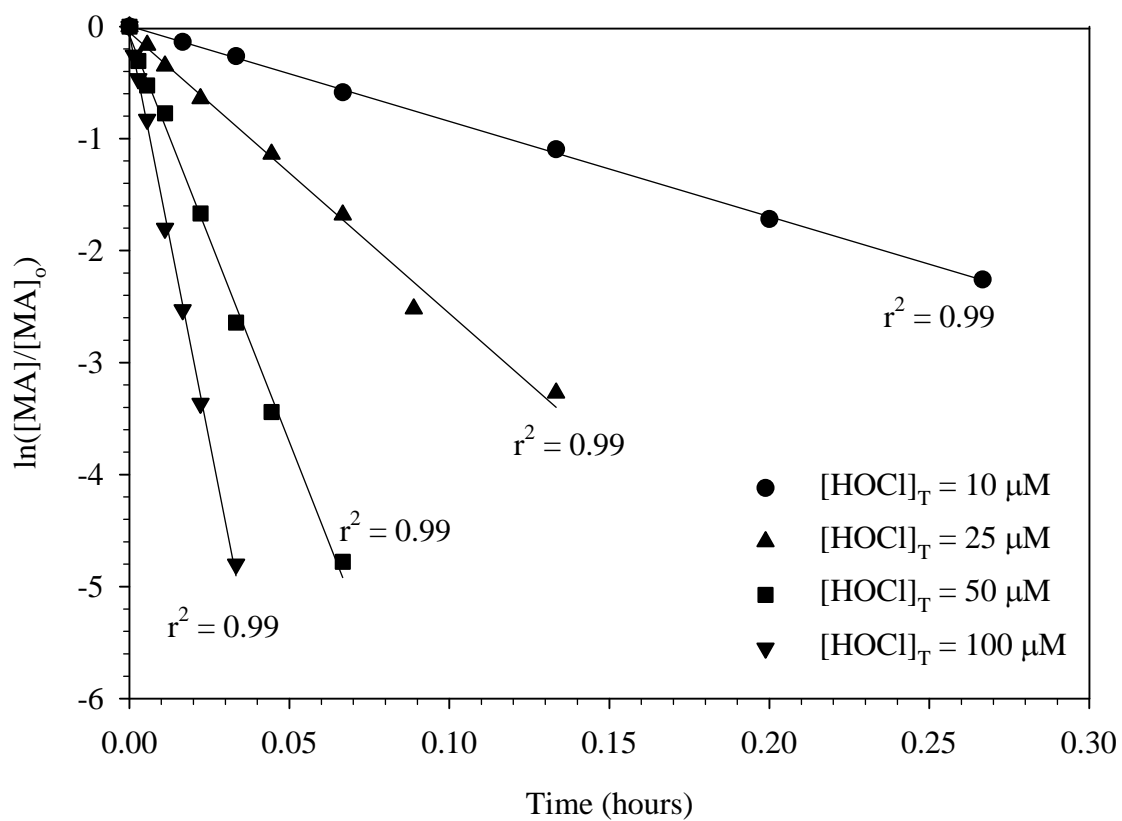


Figure 7 Observed first-order rate of MA loss in the presence of aqueous chlorine at pH 6.5.  $[MA]_0 = 0.5 \mu M$ ,  $[HOCl]_0 = 10-100 \mu M$ ,  $[PO_4]_T = 10 \text{ mM}$ , and Temperature =  $25 \pm 1^\circ C$ . Experiments performed in triplicate.

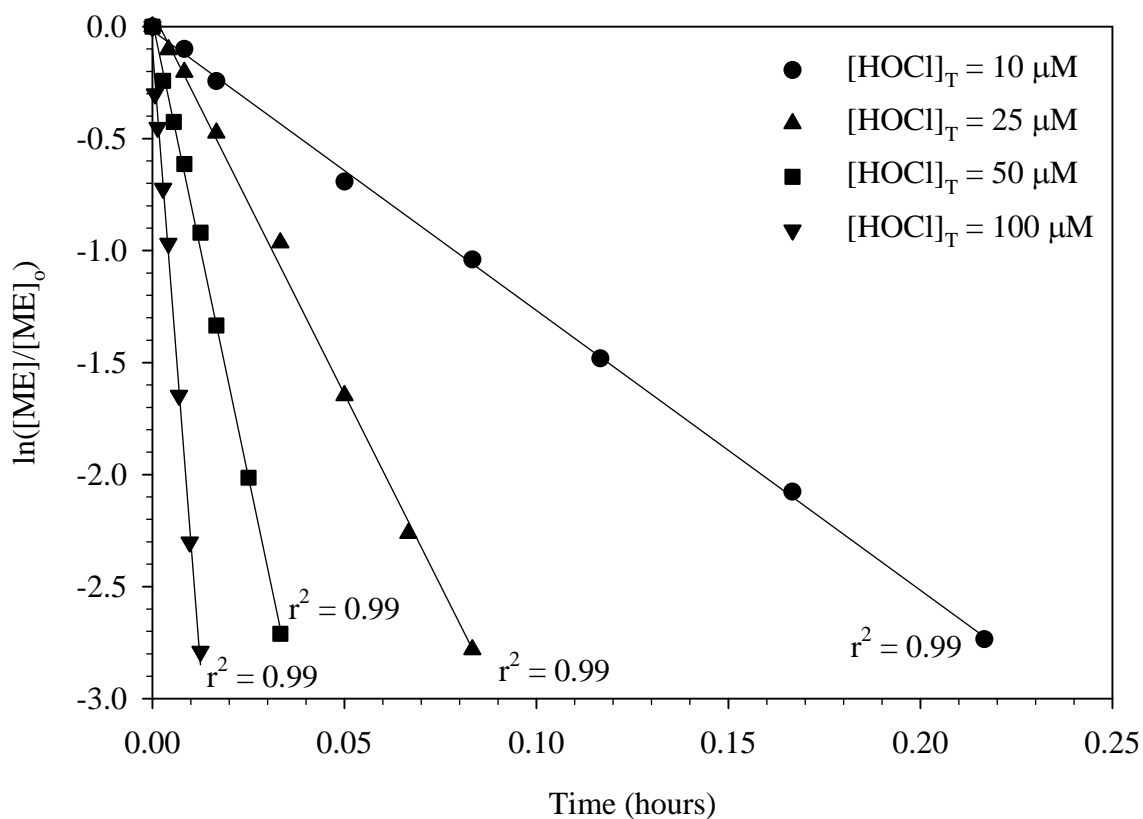


Figure 8 Observed first-order rate of ME loss in the presence of aqueous chlorine at pH 6.5.  $[ME]_0 = 0.5 \mu M$ ,  $[HOCl]_0 = 10\text{-}100 \mu M$ ,  $[PO_4]_T = 10 \text{ mM}$ , and Temperature =  $25 \pm 1^\circ C$ . Experiments performed in triplicate.

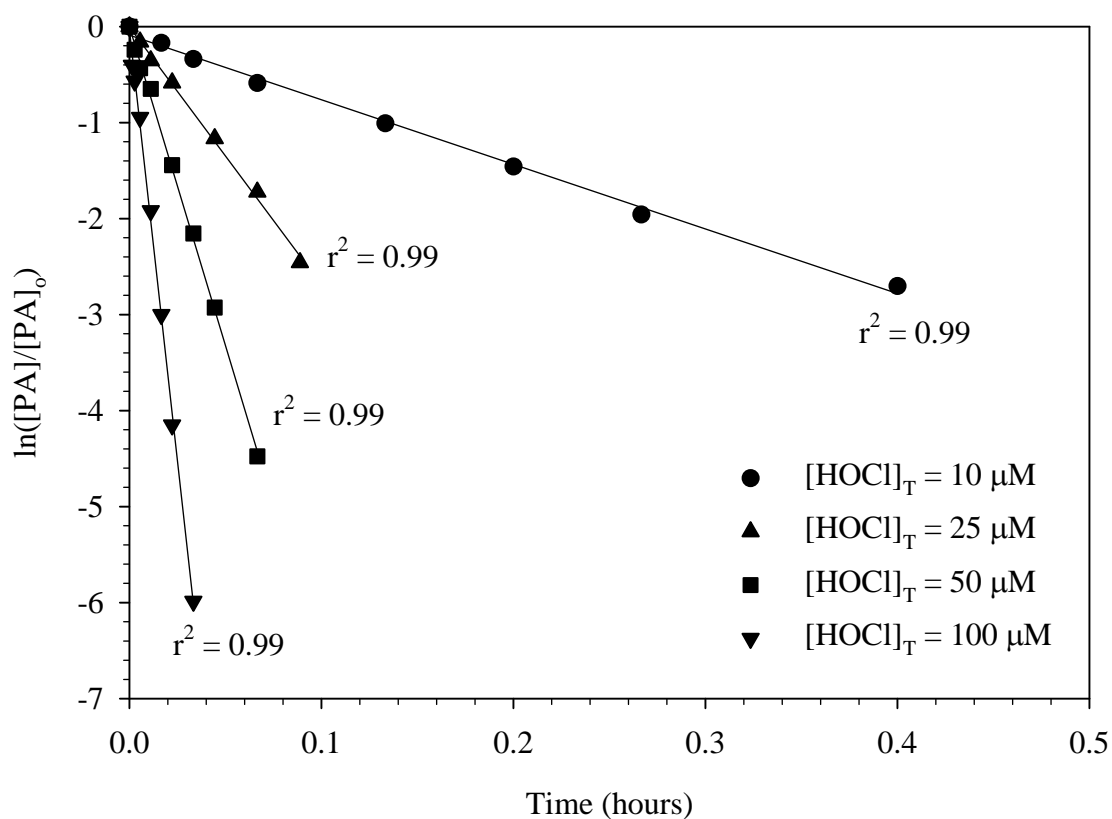


Figure 9 Observed first-order rate of PA loss in the presence of aqueous chlorine at pH 6.5.  $[PA]_0 = 0.5 \mu M$ ,  $[HOCl]_0 = 10\text{--}100 \mu M$ ,  $[PO_4]_T = 10 \text{ mM}$ , and Temperature =  $25 \pm 1^\circ C$ . Experiments performed in triplicate.

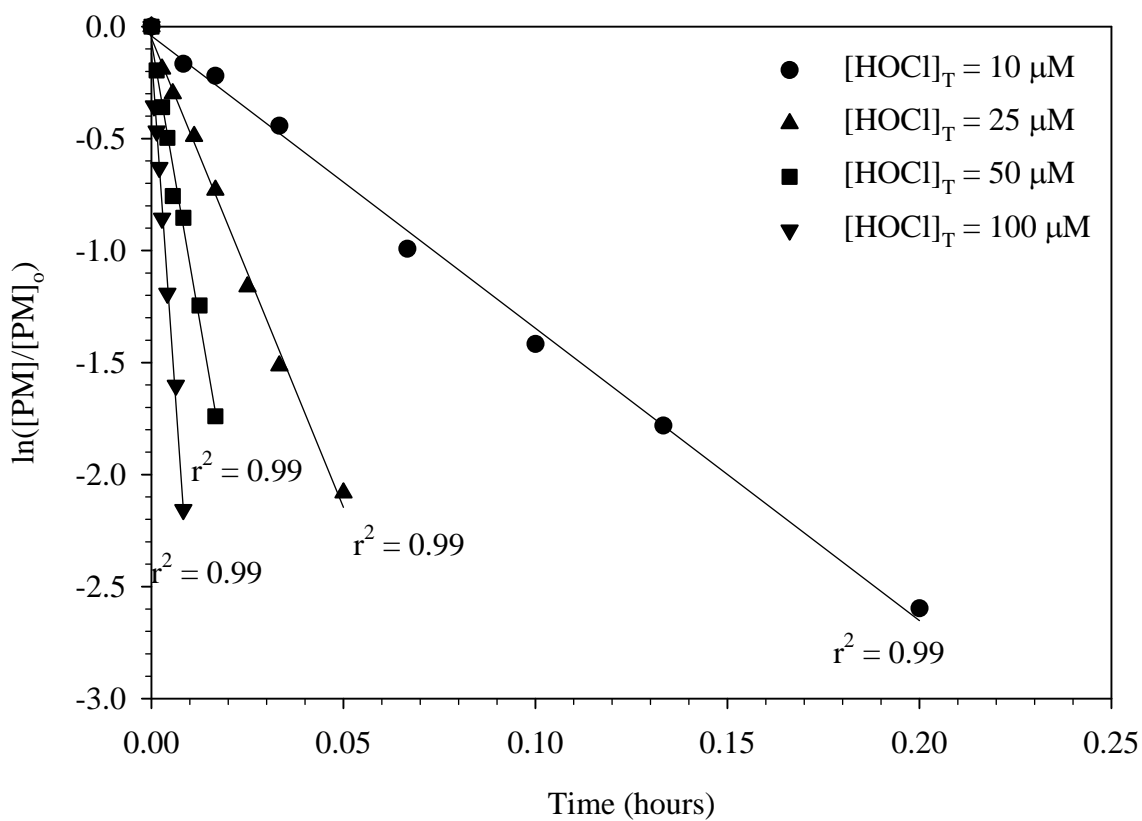


Figure 10 Observed first-order rate of PM loss in the presence of aqueous chlorine at pH 6.5.  $[PM]_0 = 0.5 \mu M$ ,  $[HOCl]_0 = 10\text{--}100 \mu M$ ,  $[PO_4]_T = 10 \text{ mM}$ , and Temperature =  $25 \pm 1^\circ C$ . Experiments performed in triplicate.

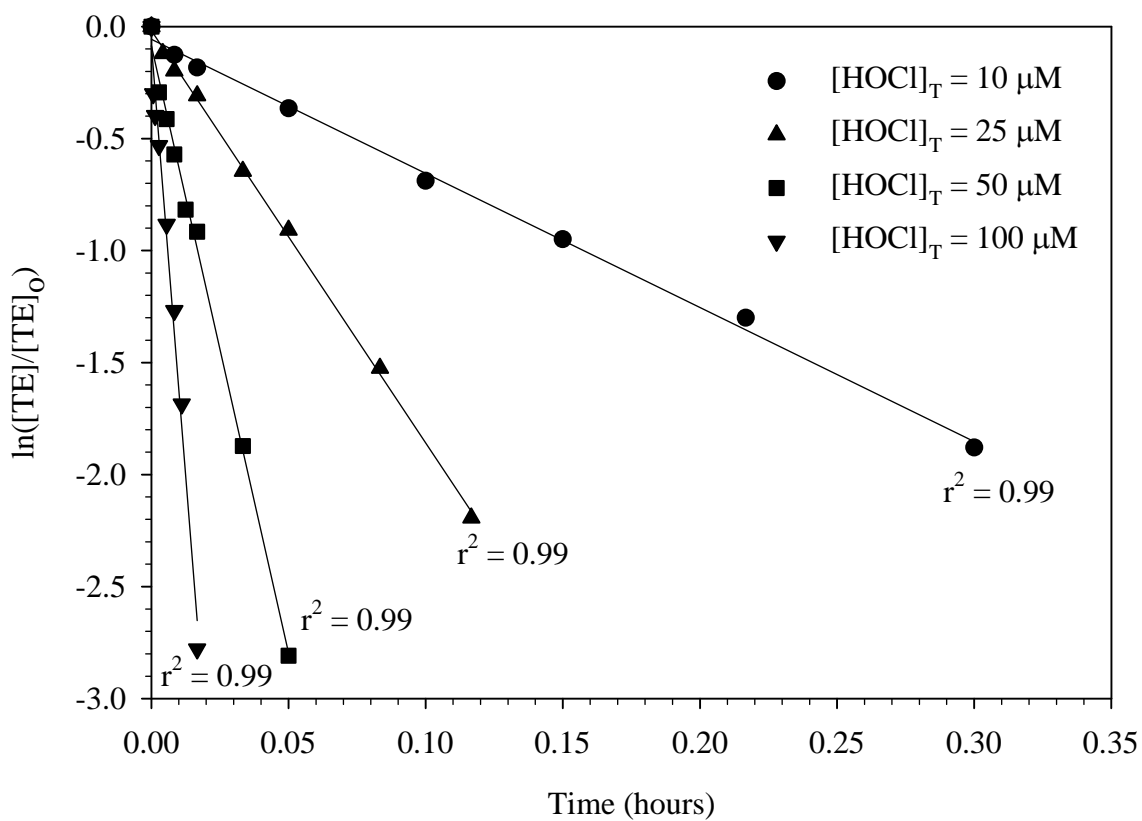


Figure 11 Observed first-order rate of TE loss in the presence of aqueous chlorine at pH 6.5.  $[TE]_0 = 0.5 \mu M$ ,  $[HOCl]_0 = 10\text{-}100 \mu M$ ,  $[PO_4]_T = 10 \text{ mM}$ , and Temperature =  $25 \pm 1^\circ C$ . Experiments performed in triplicate.

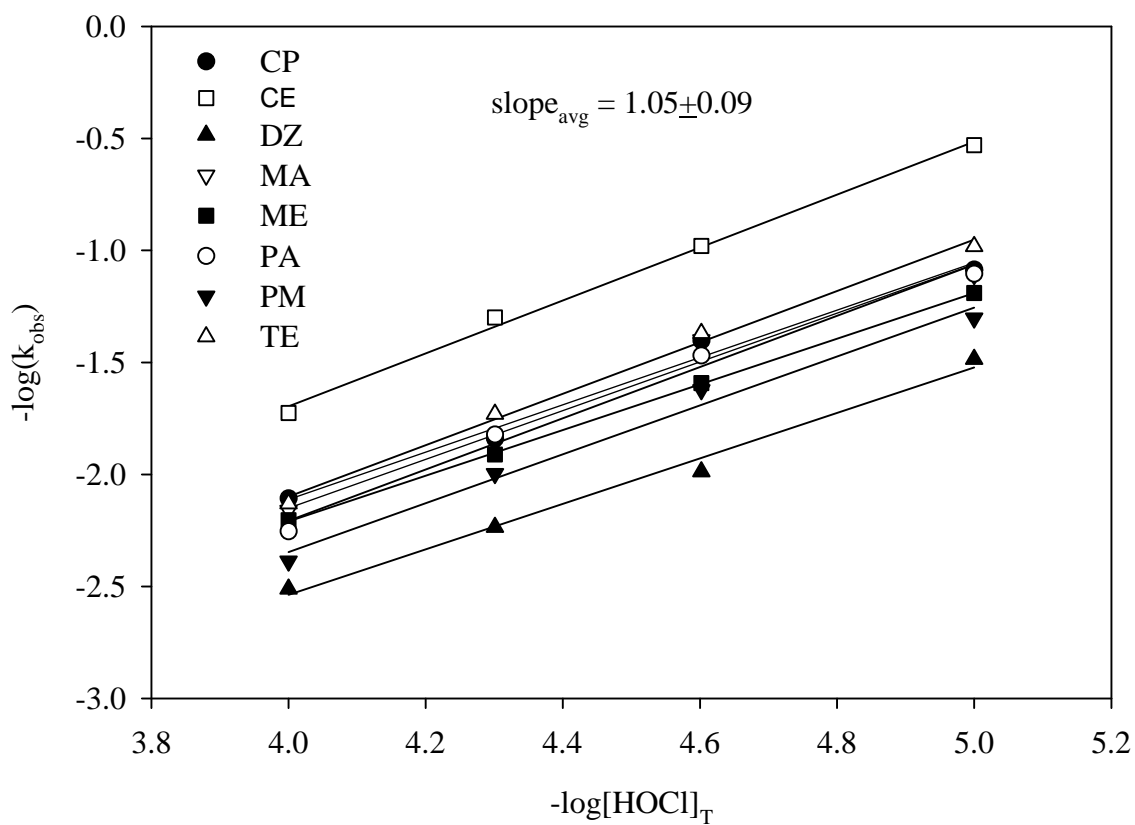


Figure 12 The reaction order of chlorine with 8 OP pesticides at pH 6.5.  $[OP]_o = 0.5 \mu\text{M}$ ,  $[PO_4]_T = 10 \text{ mM}$ , Temperature =  $25 \pm 1^\circ\text{C}$ , and  $[HOCl]_T = 10\text{-}100 \mu\text{M}$ .



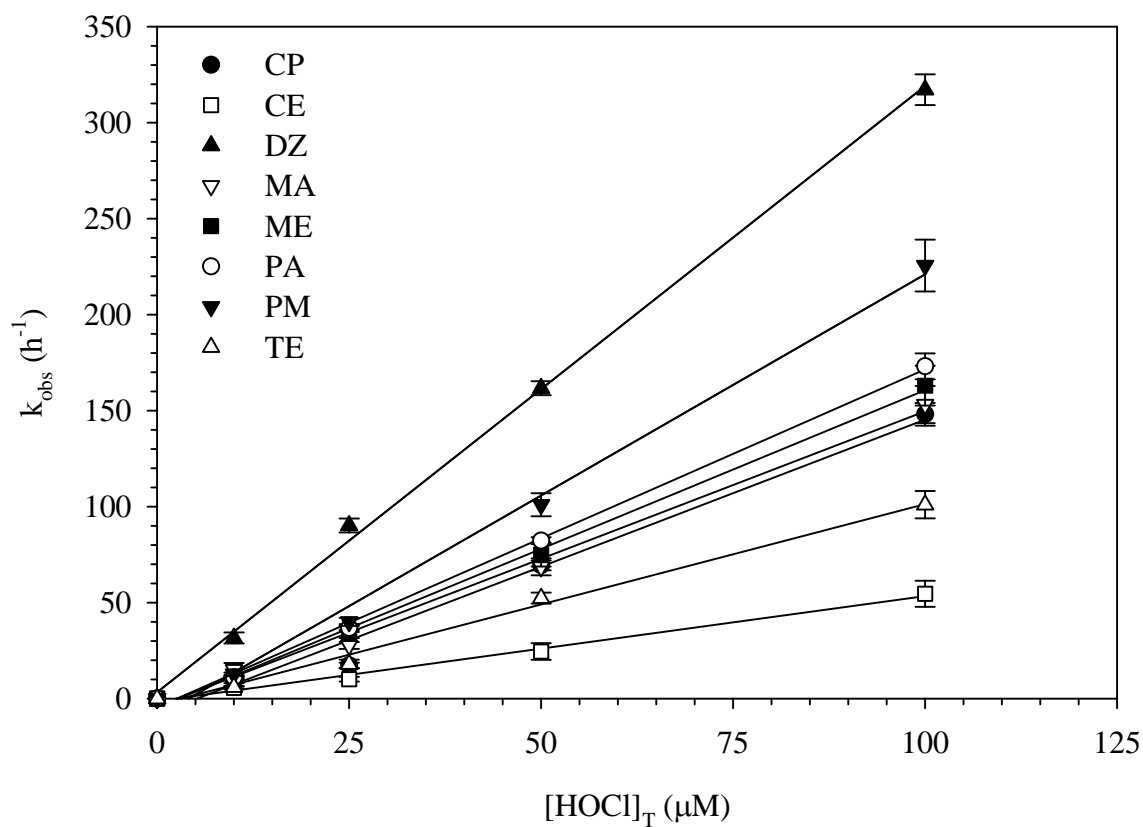


Figure 13 Second-order apparent rate coefficient for the OP pesticides at pH 6.5.  $[\text{OP}]_0 = 0.5 \mu\text{M}$ ,  $[\text{PO}_4]_{\text{T}} = 10 \text{ mM}$ , Temperature =  $25 \pm 1^\circ\text{C}$ , and  $[\text{HOCl}]_{\text{T}} = 0\text{-}100 \mu\text{M}$ . Error bars represent 95% confidence intervals.

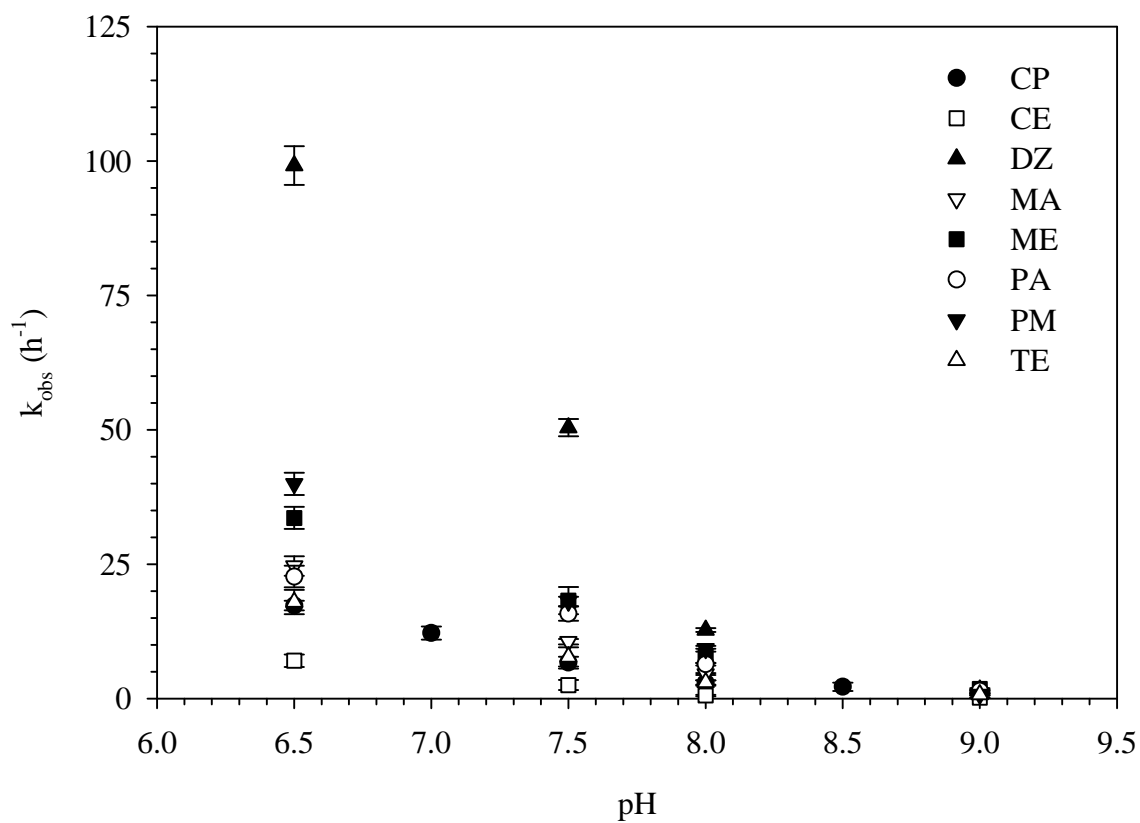


Figure 14 The pH dependency of the first-order observed rate coefficients for the OP pesticides.  $[\text{OP}]_0 = 0.5 \mu\text{M}$ ,  $[\text{HOCl}]_T = 25 \mu\text{M}$ ,  $[\text{Buffer}]_T = 10 \text{ mM}$ , and Temperature =  $25^\circ\text{C}$ . Error bars represent 95% confidence intervals.

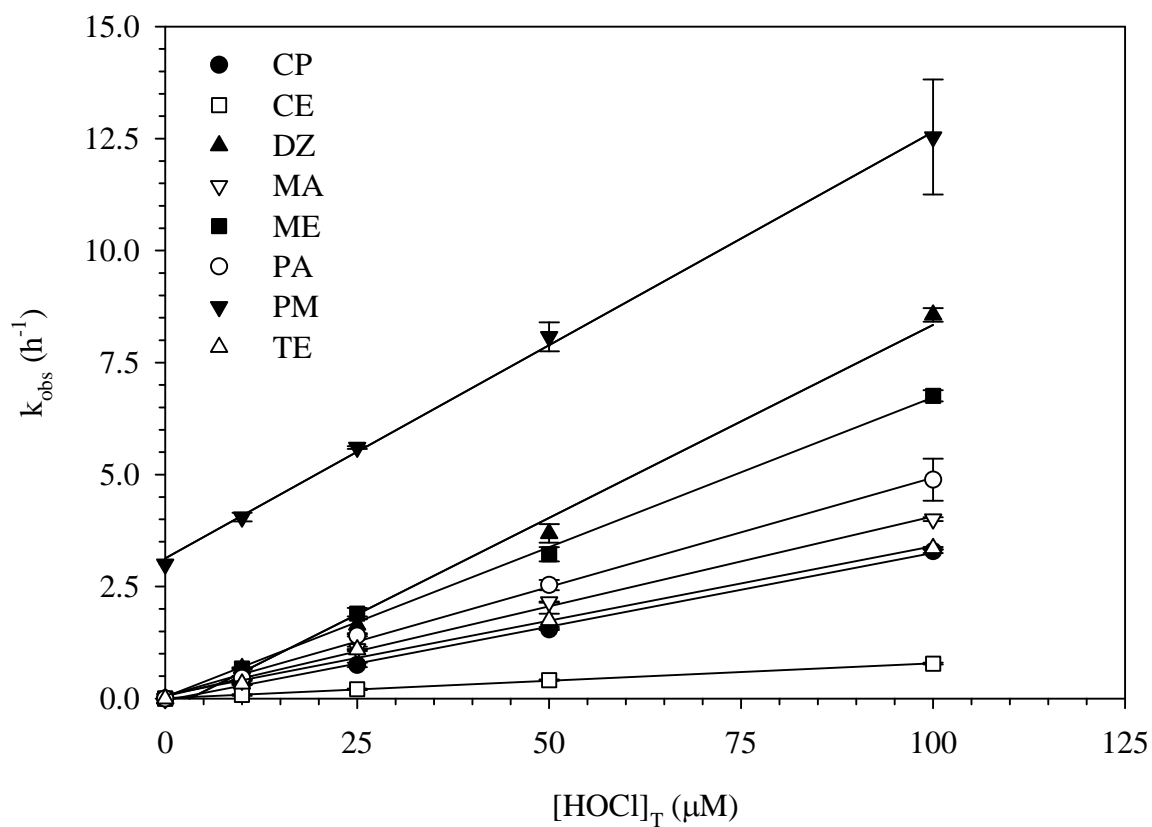


Figure 15 Second-order apparent rate coefficient for the OP pesticides at pH 9.  $[\text{OP}]_0 = 0.5 \mu\text{M}$ ,  $[\text{CO}_3]_{\text{T}} = 10 \text{ mM}$ , Temperature =  $25 \pm 1^\circ\text{C}$ , and  $[\text{HOCl}]_{\text{T}} = 0\text{--}100 \mu\text{M}$ . Error bars represent 95% confidence intervals.

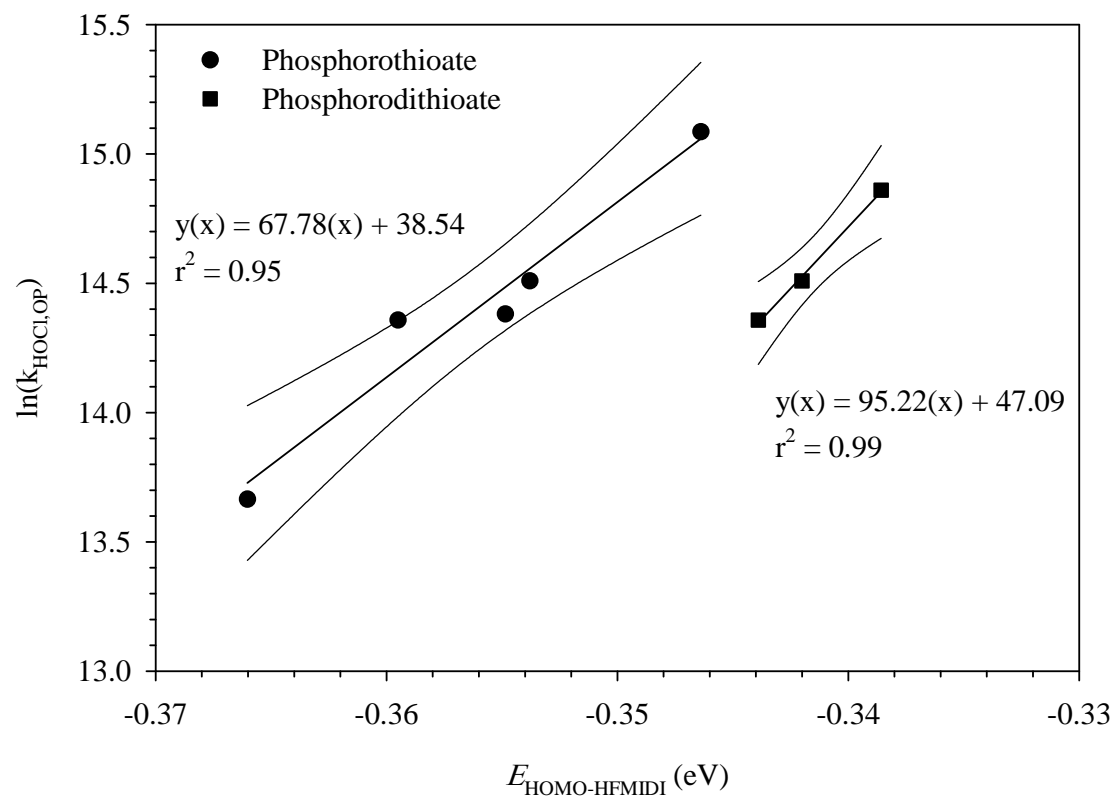


Figure 16 Relationship between the  $k_{\text{HOCl,OP}}$  with  $E_{\text{HOMO}}$  as a function of OP pesticide subgroup. Error bars about the regression line represent 95% confidence intervals.

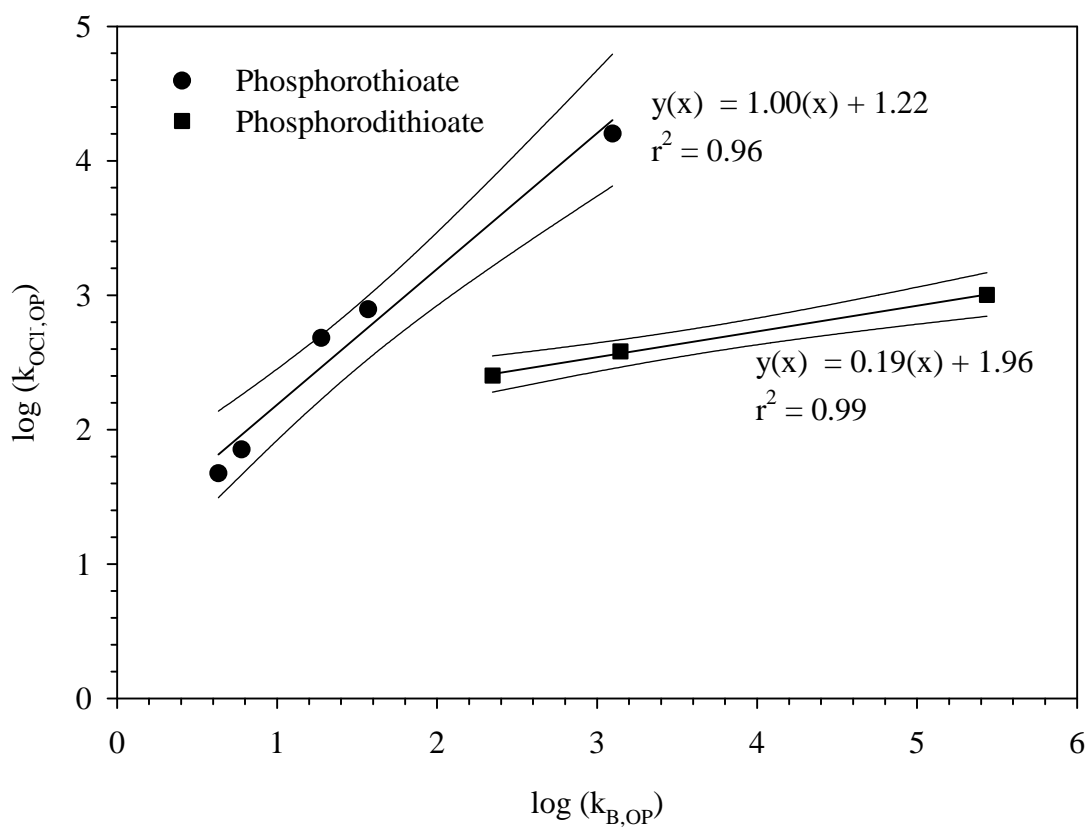


Figure 17 Relationship between the  $k_{\text{OCl,OP}}$  with alkaline hydrolysis rate coefficient as a function of OP pesticide subgroup. Error bars about the regression line represent 95% confidence intervals.

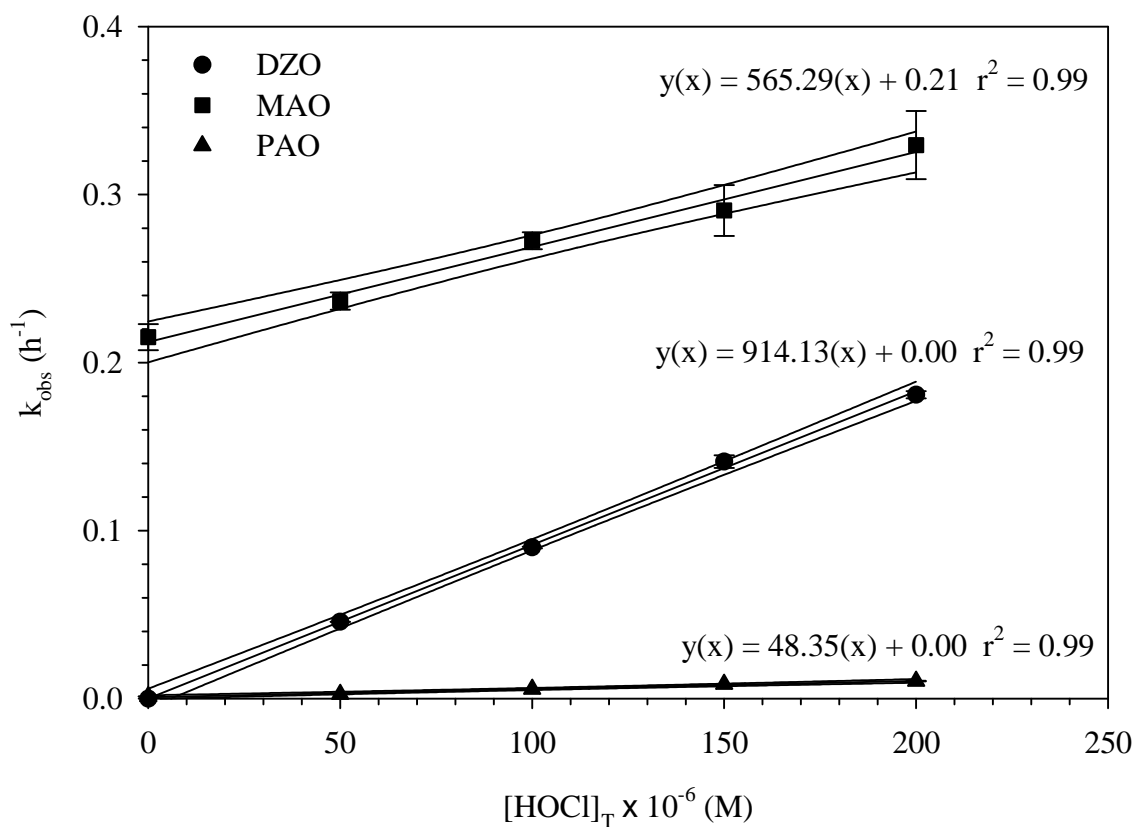


Figure 18 Second-order apparent rate coefficient of 3 OP pesticide oxons at pH 9.  $[\text{OP}]_{\text{o}} = 0.5 \mu\text{M}$ ,  $[\text{CO}_3]_{\text{T}} = 10 \text{ mM}$ , Temperature =  $25 \pm 1^\circ\text{C}$ , and  $[\text{HOCl}]_{\text{T}} = 0\text{-}200 \mu\text{M}$ . Error bars represent 95% confidence intervals for both data points and regression lines.

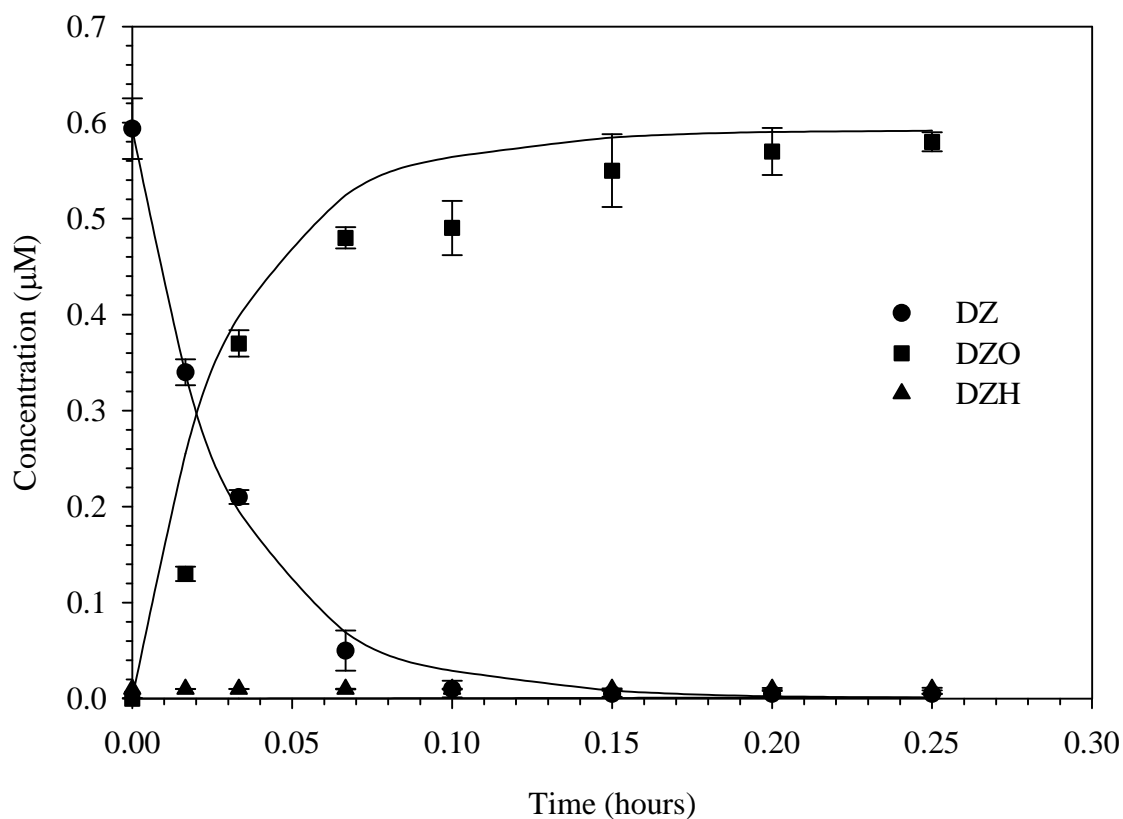


Figure 19 Experimental and model results for DZ loss in the presence of chlorine at pH 7.0.  $[DZ]_0 = 0.6 \mu\text{M}$ ,  $[HOCl]_T = 20 \mu\text{M}$ ,  $[PO_4]_T = 10 \text{ mM}$ , and Temperature =  $25 \pm 1^\circ\text{C}$ . Error bars represent 95% confidence intervals. Lines represent model results.

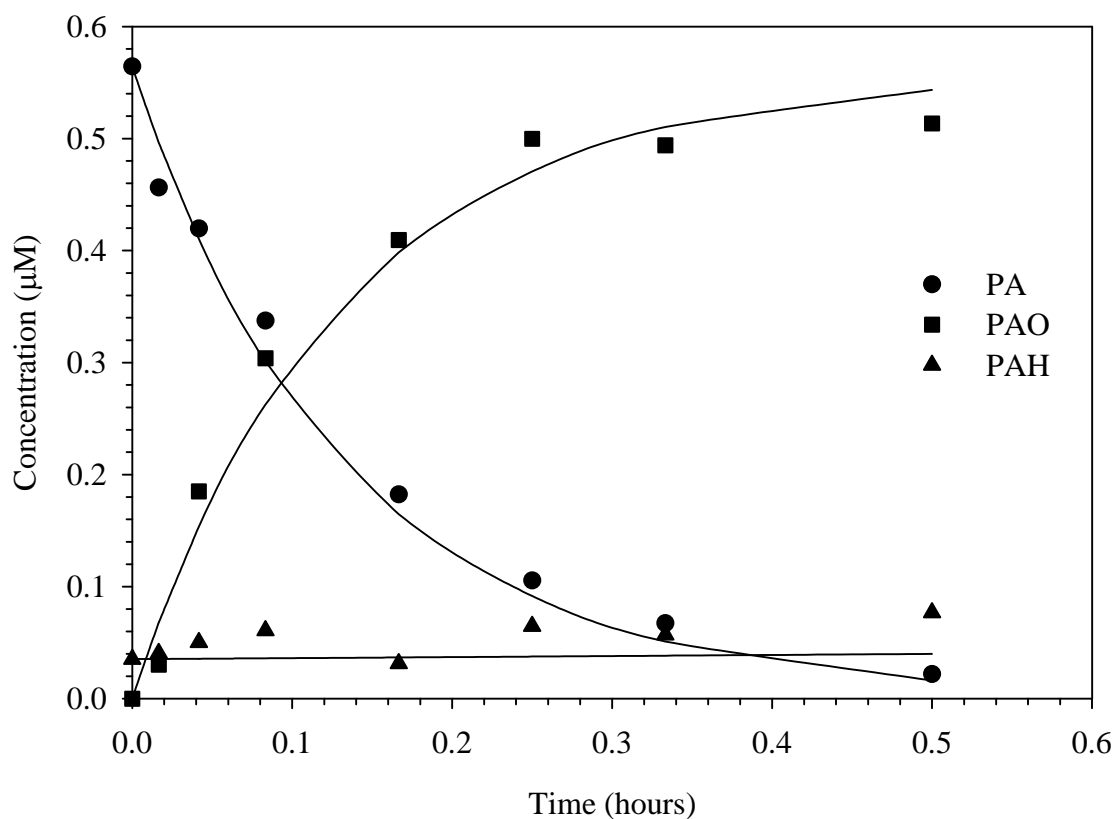


Figure 20 Experimental and model results for PA loss in the presence of chlorine at pH 8.0.  $[PA]_0 = 0.57 \mu\text{M}$ ,  $[HOCl]_T = 25 \mu\text{M}$ ,  $[PO_4]_T = 10 \text{ mM}$ , and Temperature =  $25 \pm 1^\circ\text{C}$ . Lines represent model results.



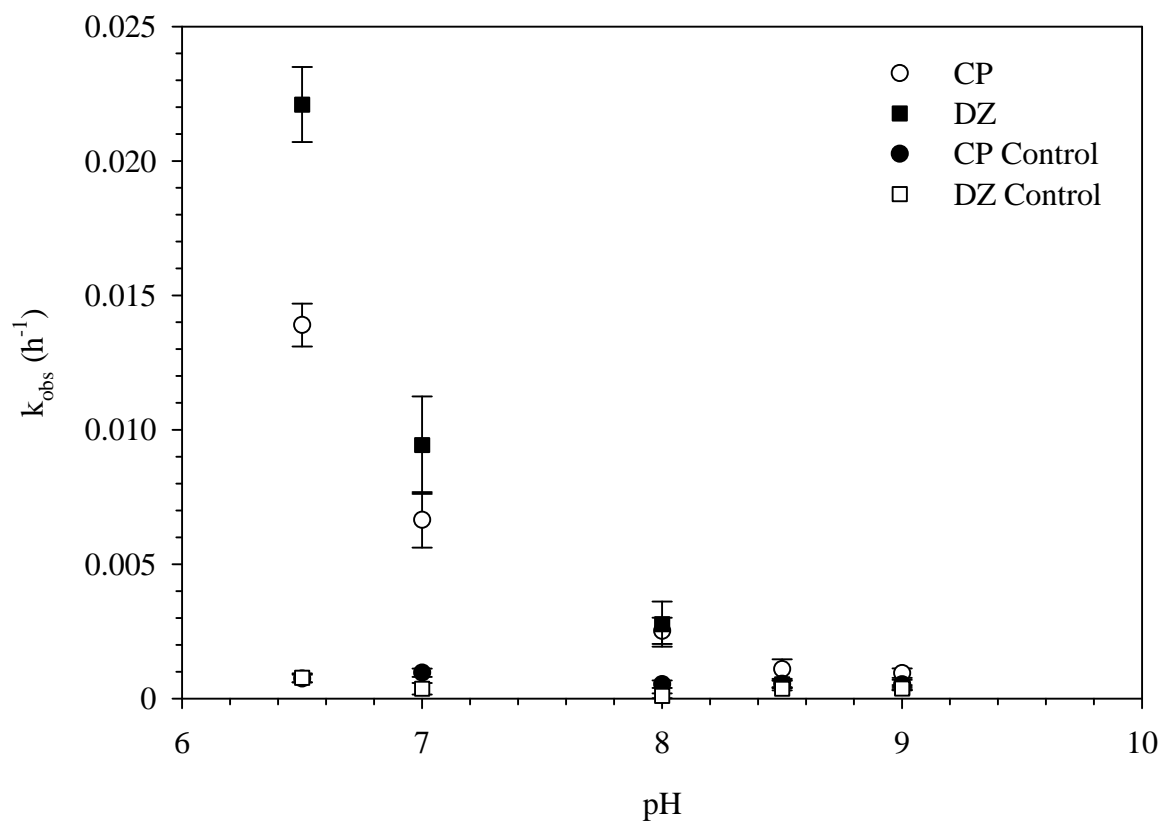


Figure 21 First-order observed loss of CP and DZ in the presence of monochloramine as a function of pH.  $[NH_2Cl] = 50 \mu M$ ,  $[OP]_0 = 0.5 \mu M$ ,  $Cl/N = 0.7 \text{ mol/mol}$ ,  $[Buffer]_T = 10 \text{ mM}$ , Temperature =  $25 \pm 1^\circ C$ , and pH 6.5-9.0. Error bars represent 95% confidence intervals.

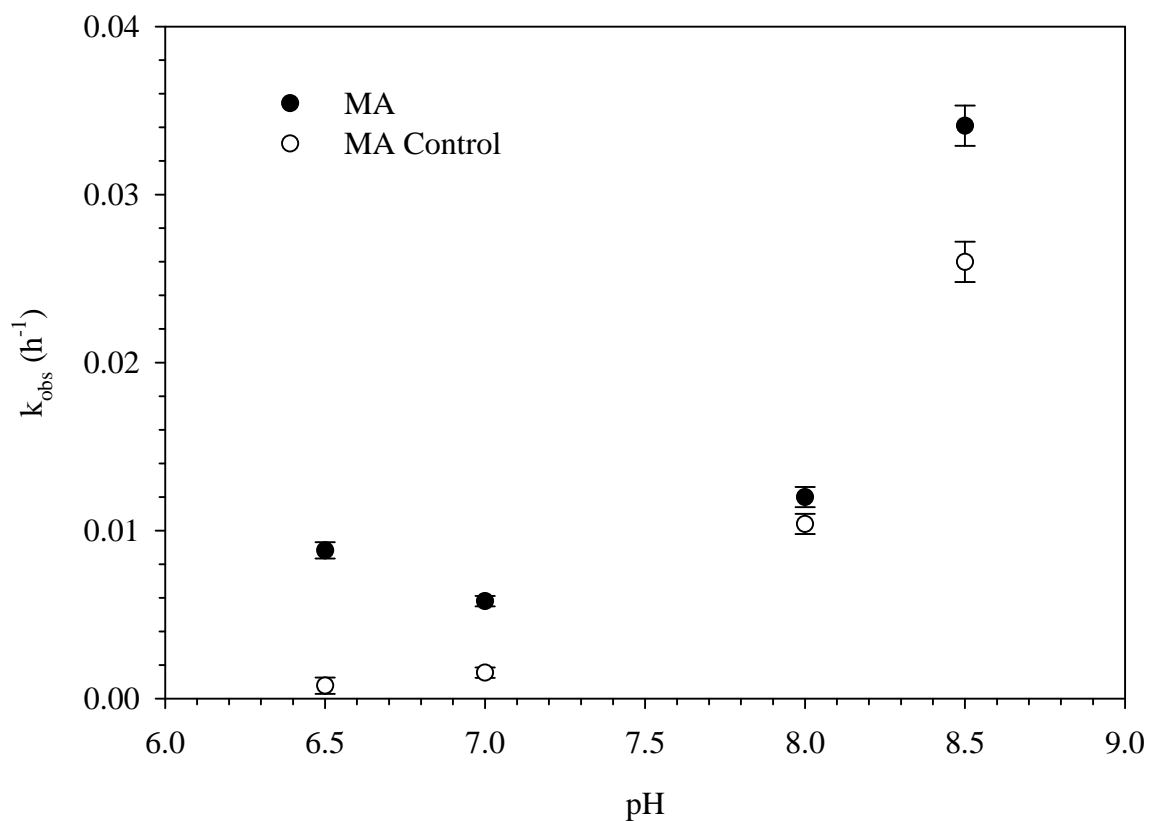


Figure 22 First-order observed loss of MA in the presence of monochloramine as a function of pH.  $[\text{NH}_2\text{Cl}] = 50 \mu\text{M}$ ,  $[\text{MA}]_0 = 0.5 \mu\text{M}$ ,  $\text{Cl/N} = 0.7 \text{ mol/mol}$ ,  $[\text{Buffer}]_{\text{T}} = 10 \text{ mM}$ , Temperature =  $25 \pm 1^\circ\text{C}$ , and pH 6.5-9.0. Error bars represent 95% confidence intervals.

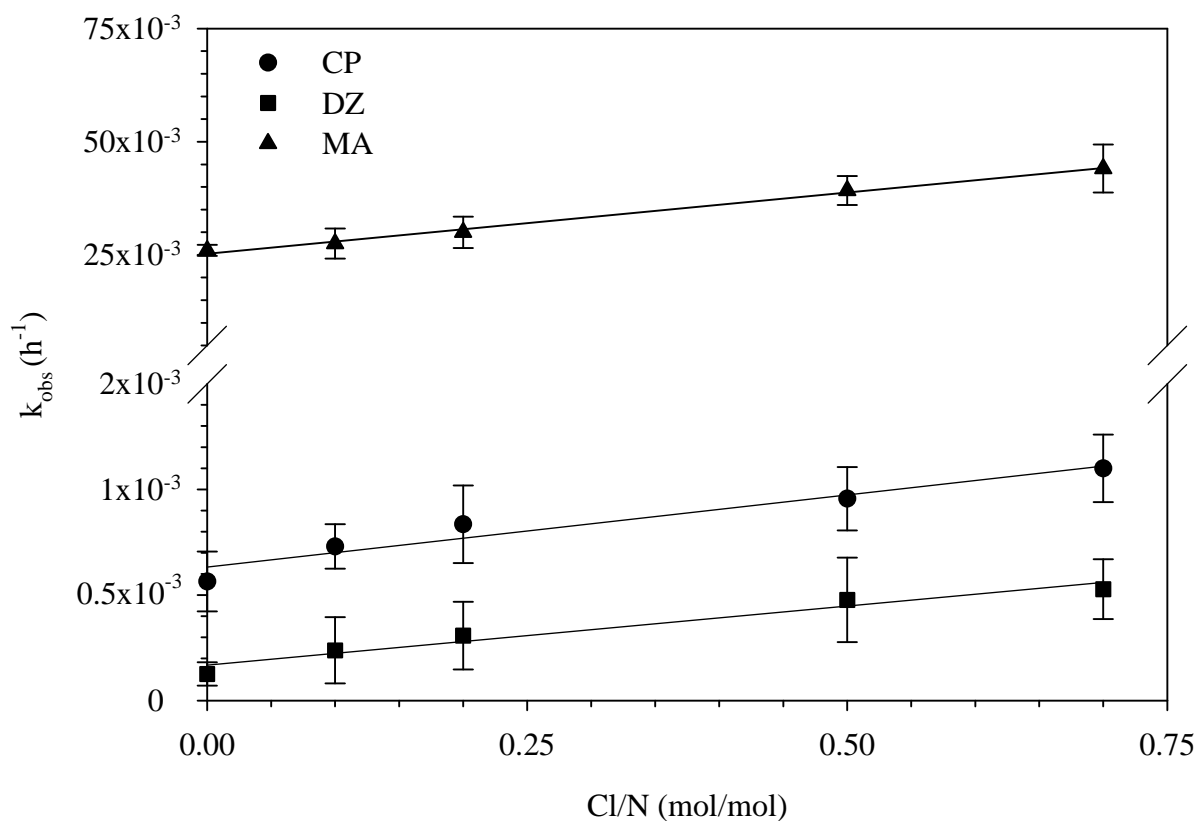


Figure 23 Observed first-order observed loss of three OP pesticides in the presence of monochloramine at pH 8.5.  $[NH_2Cl] = 50 \mu M$ ,  $[OP]_0 = 0.5 \mu M$ ,  $Cl/N = 0-0.7$  mol/mol,  $[H_3BO_3]_T = 10$  mM, and Temperature =  $25 \pm 1^\circ C$ . Error bars represent 95% confidence intervals.

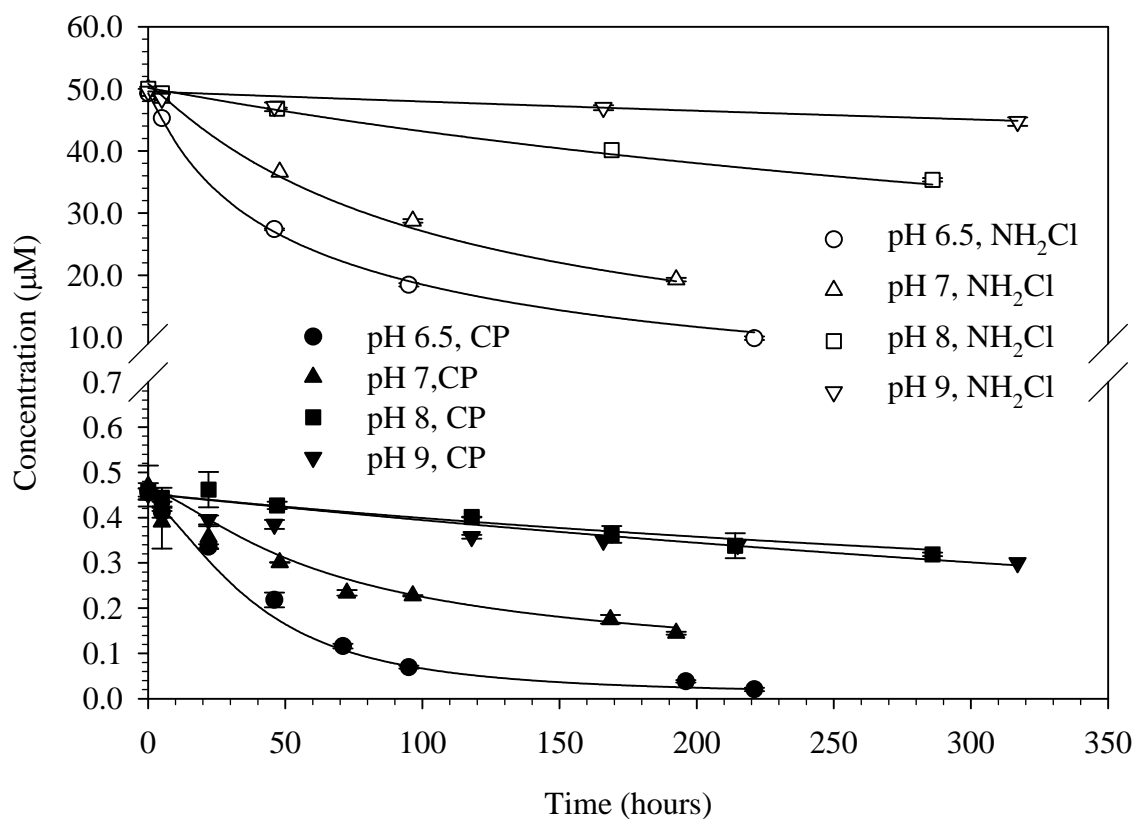


Figure 24 Experimental and model results for CP loss in the presence of monochloramine.  $[CP]_0 = 0.5 \mu\text{M}$ ,  $[NH_2Cl]_0 = 50 \mu\text{M}$ ,  $Cl/N = 0.7 \text{ mol/mol}$ ,  $[Buffer]_T = 10 \text{ mM}$ , pH 6.5-9, and Temperature =  $25 \pm 1^\circ\text{C}$ . Error bars represent 95% confidence intervals. Lines represent model results.

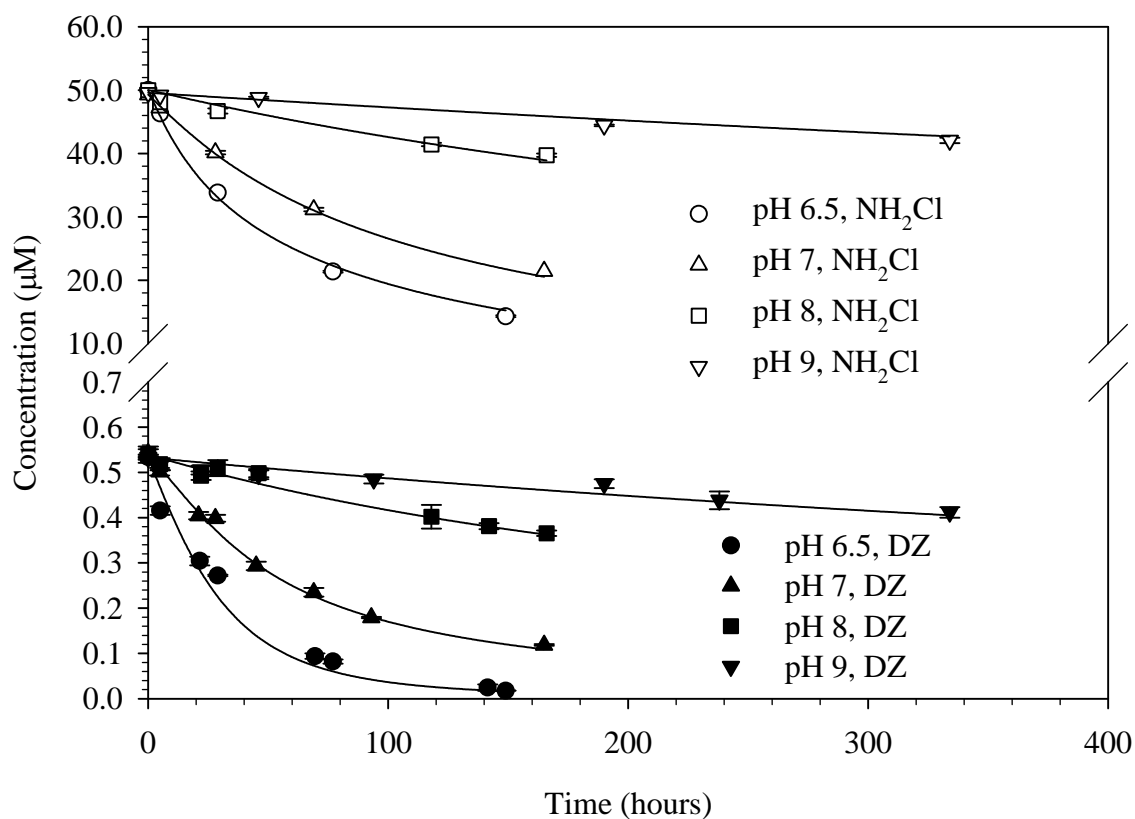


Figure 25 Experimental and model results for DZ loss in the presence of monochloramine.  $[\text{DZ}]_0 = 0.5 \mu\text{M}$ ,  $[\text{NH}_2\text{Cl}]_0 = 50 \mu\text{M}$ ,  $\text{Cl}/\text{N} = 0.7 \text{ mol/mol}$ ,  $[\text{Buffer}]_T = 10 \text{ mM}$ , pH 6.5-9, and Temperature =  $25 \pm 1^\circ\text{C}$ . Error bars represent 95% confidence intervals. Lines represent model results.

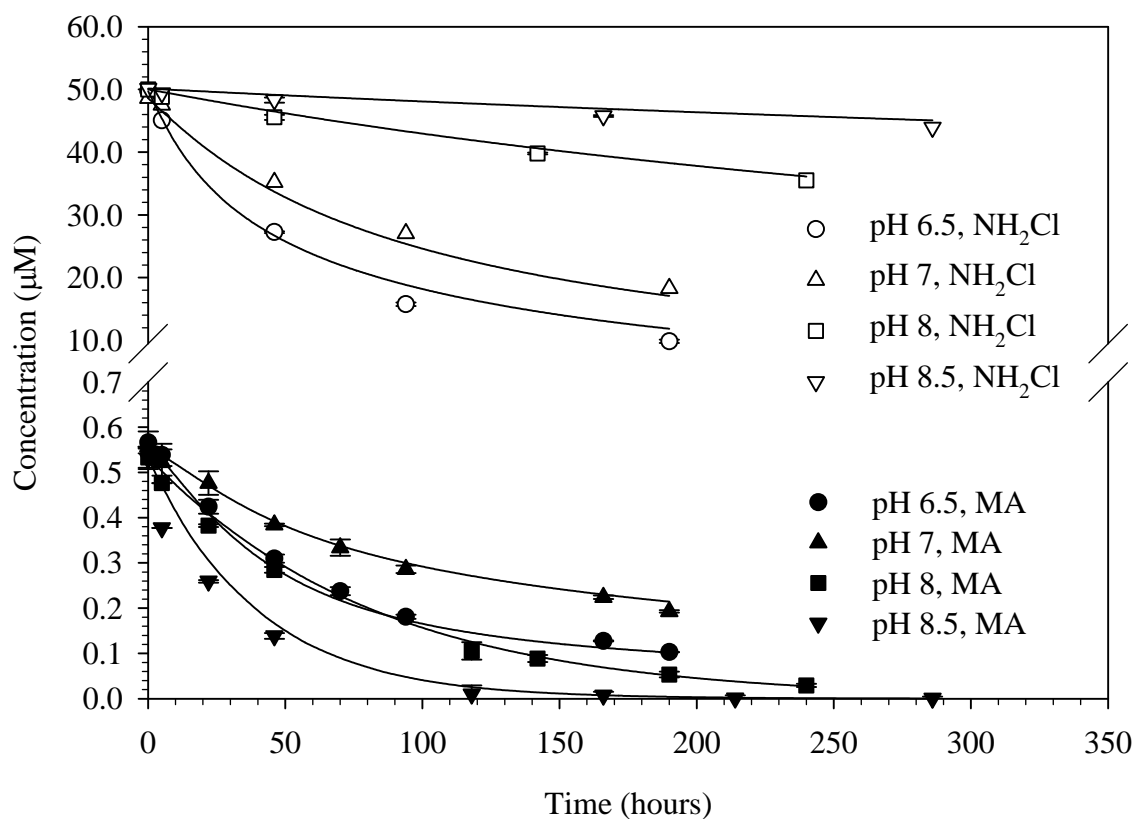


Figure 26 Experimental and model results for MA loss in the presence of monochloramine.  $[\text{MA}]_0 = 0.5 \mu\text{M}$ ,  $[\text{NH}_2\text{Cl}]_0 = 50 \mu\text{M}$ ,  $\text{Cl}/\text{N} = 0.7 \text{ mol/mol}$ ,  $[\text{Buffer}]_T = 10 \text{ mM}$ , pH 6.5-8.5, and Temperature =  $25 \pm 1^\circ\text{C}$ . Error bars represent 95% confidence intervals. Lines represent model results.

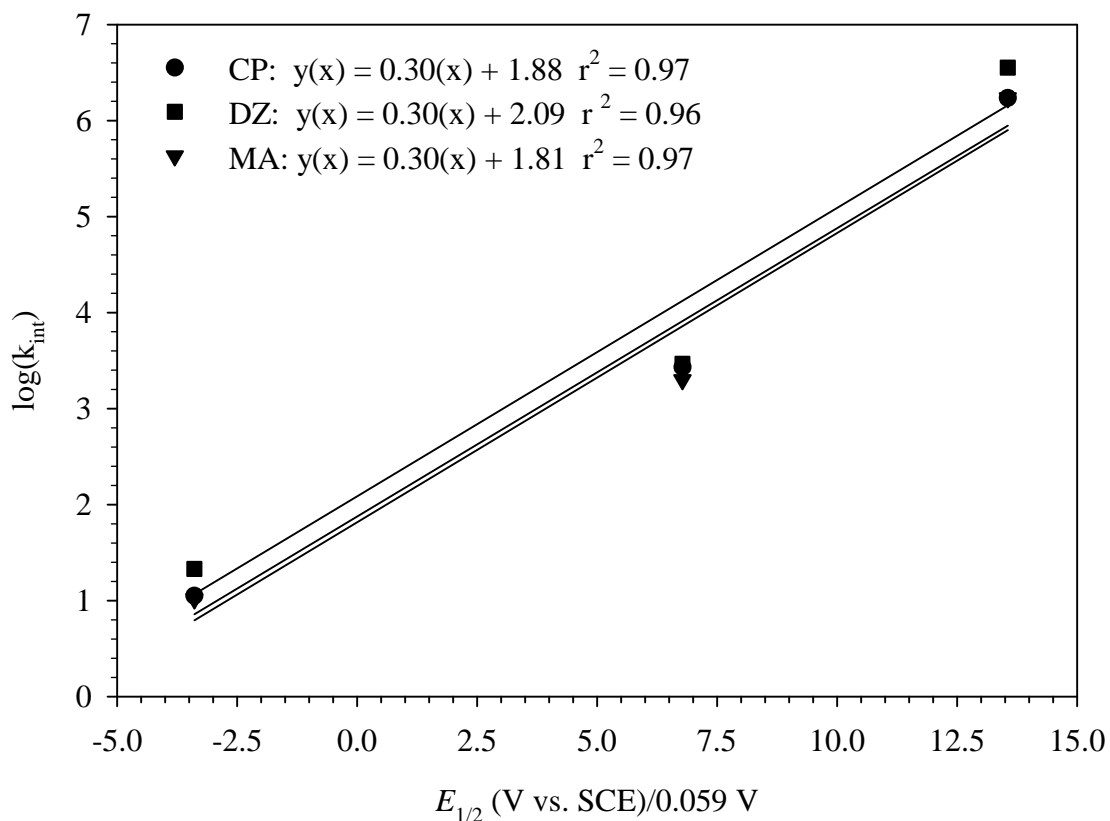


Figure 27 Structure-activity relationship relating the reaction of monochloramine, dichloramine, and hypochlorous acid with CP, DZ, and MA. Piela and Wrona (49) found half-wave potentials for monochloramine (-0.2 V), dichloramine (0.4), and hypochlorous acid (0.8 V). These values were then converted using the Nernst equation to the intensive property of the log ratio of the activities of the reduced products to the oxidized forms of the oxidant.



United States  
Environmental Protection  
Agency

Office of Research  
and Development (8101R)  
Washington, DC 20460

Official Business  
Penalty for Private Use  
\$300

EPA 600/R-08/089  
September 2008

Please make all necessary changes on the below label,  
detach or copy, and return to the address in the upper  
left-hand corner.

If you do not wish to receive these reports CHECK HERE

☐; detach, or copy this cover, and return to the address in  
the upper left-hand corner.

PRESORTED STANDARD  
POSTAGE & FEES PAID  
EPA  
PERMIT No. G-35



**Recycled/Recyclable**  
Printed with vegetable-based ink on  
paper that contains a minimum of  
50% post-consumer fiber content  
processed chlorine free